



Does parameterization affect the complexity of agent-based models?

Jiri Kukacka^{a,b,*}, Ladislav Kristoufek^{a,b}

^a Czech Academy of Sciences, Institute of Information Theory and Automation, Pod Vodarenskou vezi 4, Prague 8 182 00, Czechia

^b Charles University, Faculty of Social Sciences, Institute of Economic Studies, Opletalova 26, Prague 1 110 00, Czechia

ARTICLE INFO

Article history:

Received 17 July 2020

Revised 30 July 2021

Accepted 1 October 2021

JEL classification:

C13

C22

C63

D84

G02

G17

Keywords:

Financial agent-based models

Parameterization

Complex systems

Multifractal sensitivity analysis

Detrended fluctuation analysis

ABSTRACT

We examine the complexity of financial returns generated by popular agent-based models through studying multifractal properties of such time series. Specifically, we are interested in the sensitivity of the models to their parameter settings and whether some patterns emerge in the connection between complexity and a specific type of parameter. We find that (i) herding behavior mostly boosts the model complexity as measured by multifractality, (ii) various in-built stabilizing factors increase model complexity, while (iii) the role of the intensity of choice, the number of agents, as well as the chartists' representation have rather model-specific effects. Finally, the core feature driving the model complexity seems to be the implementation of a switching mechanism governing agents' interactions. The heterogeneous set of nine analyzed models thus offers some universal concepts that hold across their range. Our results also indicate that complex dynamics are observed not only for the benchmark parameter settings but also for other combinations of parameter values for most models. This opens new avenues for future research and specifically motivates examining the models in more detail by focusing on other dynamic properties in addition to the herein presented multifractality.

© 2021 Elsevier B.V. All rights reserved.

1. Introduction

Financial agent-based models (LeBaron, 2006; Hommes, 2006; Chen et al., 2012; Dieci and He, 2018) have not only successfully proven their replication abilities of the stylized facts of financial time series but have also allowed for a more elaborate analysis of the link between their design and the system dynamic properties they generate. The former might include both the theoretical derivation of the models as well as a specific setup of parameter calibration. Even though the topical literature has rather moved from constructing more complicated models toward their estimation (Fagiolo et al., 2007; Windrum et al., 2007; Grazzini et al., 2017; Lux and Zwinkels, 2018; Lux, 2018; Fagiolo et al., 2019; Platt, 2020), the discussion of the model parameter sensitivity is usually lacking, and the models are often introduced with either one or a limited number of parameter settings showing only the stylized behavior of the data they generate. However, a more detailed insight into such sensitivity will help to understand the often-complicated dynamics of these models, not only for the purposes of interpretation and possible policy implications but also to support selection of proper tools and instruments for the model estimation. Deciding whether to use likelihood-based estimation methods for a given model when observing

* Corresponding author.

E-mail addresses: kukacka@utia.cas.cz (J. Kukacka), kristoufek@utia.cas.cz (L. Kristoufek).

multiple local maxima of the metrics for a perceived optimal parameter setting of such model is a typical example of such dilemma. Naturally, as the agent-based models are defined through a set of parameters and there are many possible outputs of interest that describe the dynamics of the generated series, the problem at hand becomes highly multidimensional. One thus needs to be rather strict in at least one of the dimensions to make the task not only feasible but also understandable and presentable. In a similar vein, the generated series, usually financial returns, can be described in variety of ways and their dynamic properties can be characterized by many statistics and measures.

In this paper, we build on the flexibility of the financial agent-based models to disentangle effects that can lead to the multifractal behavior of financial time series. We focus on multifractality as a nontrivial feature of financial series that is frequently studied empirically (Lux and Kaizoji, 2007; Zhou, 2009; Barunik et al., 2012), but its interpretation and connection to the markets' characteristics have been quite limited. Partially building on the fractional generalizations of autoregressive moving average processes (ARFIMA/FARIMA, going back to Mandelbrot and Van Ness (1968)), which are traditional instruments for modeling financial returns, multifractality allows for complicated scaling of moments in the process dynamics. To better describe such complex behavior, various models have been proposed, such as the multifractal random walk (Bacry et al., 2001), the Markov-Switching Multifractal (Calvet and Fisher, 2001), and the multifractal model of asset returns (Calvet and Fisher, 2002; Lux, 2004) leading to multifrequency approaches to the news arrival into asset pricing (Calvet and Fisher, 2007) as well as asset pricing and risk sharing based on an aggregation of heterogeneous beliefs (Calvet et al., 2018). It has also been connected to critical and extreme events on the financial markets (Lux and Ausloos, 2002; Siokis, 2017). Being a unique phenomenon connected to various specifics of the financial markets and the processes they generate, multifractality is a straightforward metric that offers a unique opportunity to study the effect of specific parameter settings on complex dynamics of the generated time series (Ivanov et al., 2001; Shimizu et al., 2002; Lopes and Betrouni, 2009).

In addition, multifractality and agent-based models form a natural pair as multifractality and multiscaling emerge through heterogeneous perception of information flows. These can be possibly represented by multiplicative cascades forming the basis for multifractal behavior of financial series (Calvet and Fisher, 2002) but mostly directing towards frequency-specific, and thus investment horizon specific, interpretation of shocks and fundamental information of the pricing process of financial assets and their risk premia as well as frequent switching within the pricing dynamics. This again resembles the typical structure of agent-based models with agents changing their investment strategies (Calvet and Fisher, 2008). Emergence of the multifractal dynamics in data generated by the agent-based models is thus at hand. By connecting the financial agent-based models with the multifractal framework, we check whether and how the multifractal features of the time series generated by these models of financial markets react to changes with respect to their parameters governing, e.g., the switching between trading strategies, herding behavior, the number of agents in the model, and others. Even though there are other possibilities of measuring the complexity of time series, mostly derived from or built on various entropy measures that are also often used in other agent-based models contexts such as goodness-of-fit measures (Gonzales Andino et al., 2000; Torres and Gamero, 2000; Chen et al., 2009; Marks, 2013; Barde, 2016; 2017; Lamperti, 2018a; 2018b), fractal and multifractal measures have been put under higher scrutiny concerning specific properties of financial time series—the financial 'stylized facts' (Cont, 2001)—and their properties have been heavily studied and understood as reviewed by Jiang et al. (2019), at least compared to the other methods.

Each agent-based model we focus on is subjected to a unified simulation-based sensitivity analysis in which we study how multifractal properties of the model-generated series react to varying parameter settings and whether intuitive patterns of the relationship can be generalized over the utilized scale. Taking advantage of the simulation-based approach, we circumvent the issues of empirical estimation (LeBaron and Tesfatsion, 2008; Grazzini and Richiardi, 2015; Recchioni et al., 2015). A grid strategy of analyzed setups together with the statistical robustness of a Monte Carlo study require advanced computational server capacities. For most models, we observe nontrivial patterns of the parameterization-complexity relationship for which we provide an overall interpretation and potential explanations. The current paper can be seen as an extension of Kukacka and Kristoufek (2020) which uncovered several specific agent-based models that can generate multifractal series in the default baseline setting. Here, we present a much more detailed study within parametrizations of each specific model, focusing on interactions and influence of different types of parameters on the multifractality strength rather than comparing the models in their baseline setting among them, thus providing a deep insight into dynamical properties of given models.

At this point, it seems important to clearly distinguish between the complexity of the models themselves and the complexity of their outputs. Via the multifractal analysis, we explicitly focus on the latter, i.e., on the "sensitivity analysis and the complexities inherent in the exploration of the space that encapsulates both the parameters and the outcomes" (Lee et al., 2015). But one might suggest that in some cases, we also implicitly/unintentionally study the former phenomenon. For instance, when varying the number of agents in the Gilli and Winker (2003) and Alfarano et al. (2008) models, we make the mutual interactions among agents less or more complicated/complex in terms of the complexity of given models. Such understanding follows the interpretation of agent-based frameworks as computational models "suitable for describing complex systems" (Mandes and Winker, 2017). The authors clearly define two dimensions of complexity: "the size of the model itself (number of components, parameters, description length, non-linearity, etc.) and the emergent complexity resulting from the aggregation of individual behavior." Therefore, it also seems crucial to distinguish between the complicatedness of a model, typical for large models with many different interactions and long simulation times, and the complexity of its output. Neither directly implies the other, especially the complexity of a model output does not directly imply the complicatedness of

the given model. Indeed, according to our analysis, even models with a straightforward structure can generate very complex output dynamics.

In the next section, we briefly introduce the technical mechanisms of the multifractal formalism and its estimation. The following section in detail describes the Monte Carlo simulation setup. What comes after are the two core sections that present the methodology and results for the nine financial agent-based models. The last section summarizes the results, presents uncovered common patterns and several apparent contradictions, and concludes with future research prospects. We find that (i) herding behavior mostly boosts the model complexity as measured by multifractality, (ii) various in-built stabilizing factors increase model complexity, while (iii) the role of the intensity of choice, the number of agents, as well as the chartists' representation have rather model-specific effects. Finally, the core feature driving the model complexity seems to be the implementation of a switching mechanism governing agents' interactions. The heterogeneous set of models we study thus offers some universal concepts that hold across their range. Supplementary material associated with this article containing R code for the MF-DFA estimator of the generalized Hurst exponent, R code for an illustrative replication of the results, and the scripts to produce the presented heat map graphics can be found on GitHub at the following address: github.com/jirikukacka/Kukacka_Kristoufek_2021 [created 2021-05-25].

2. Multifractality and its estimation

2.1. From long-range dependence to multifractality

In the time series analysis, multifractality is a property describing complex behavior of the series with respect to rich scaling of its moments. As its special case for the second moment of a series, long-range dependence (sometimes also referred to as long-term memory or persistence) is represented by a power-law behavior in its autocorrelation structure. In the frequency domain, we observe divergence of the spectrum $f(\lambda)$ at the origin so that $f(\lambda) \propto \lambda^{1-2H}$ for frequencies $\lambda \rightarrow 0+$. In the time domain, the process is characterized by an asymptotically hyperbolically decaying autocorrelation function so that $\rho(k) \propto k^{2H-2}$ for lags $k \rightarrow \pm\infty$ (Beran, 1994). The Hurst exponent H in both approaches is the characteristic parameter of such processes. For $H = 0.5$, there is no long-range dependence. Persistent processes are represented by $H > 0.5$ and anti-persistent processes by $H < 0.5$. Even though long-range dependence is usually studied only for stationary processes with the Hurst exponent between 0 and 1, the possibilities are richer and cover for instance nonstationary but still mean-reverting processes with $1 \leq H < 1.5$. A unit-root process has $H = 1.5$ that leads to the connection to the (fractional) integration parameter d so that $d = H - 0.5$ for Gaussian processes.

There are various definitions of multifractality but the one of Calvet and Fisher (2002) has become one of the most prominent and standard ones. It states that a stochastic process $\{X_t\}$ with stationary increments is multifractal as long as it holds that:

$$\mathbb{E}(|X_t|^q) \propto t^{\tau(q)+1}. \tag{1}$$

The scaling function $\tau(q)$ is linear for unifractal (monofractal) processes and concave for multifractal processes, and $q \in \mathbb{R}$ is the moment order. This connects back to the special case of long-range dependence (with $q = 2$) since the asymptotic behavior of the autocorrelation function of such process leads to a power-law scaling behavior of variance of its integrated (cumulative) series (Di Matteo et al., 2005; Di Matteo, 2007; Buonocore et al., 2016). In the language building on the long-range dependence Hurst exponent H , the generalized Hurst exponent $H(q)$ of a multifractal series can be expressed as:

$$H(q) = \frac{1 + \tau(q)}{q}. \tag{2}$$

The concave scaling function $\tau(q)$ then implies $H(q)$ decreasing in q , which in turn allows using the range of the generalized Hurst exponents as a measure of multifractality of the series in question. In natural sciences (Kantelhardt, 2009), it is more common to describe the multifractal processes through their singularity strength α and singularity spectrum $f(\alpha)$. These are defined as:

$$\alpha(q) = \frac{\partial \tau(q)}{\partial q} \text{ and } f(\alpha(q)) = q\alpha(q) - \tau(q). \tag{3}$$

The spectrum width is then used as a measure of multifractality. The connection between the generalized Hurst exponent $H(q)$ and the singularity measures is then given through:

$$\alpha(q) = H(q) + qH'(q) \text{ and } f(\alpha(q)) = q(\alpha(q) - H(q)) + 1. \tag{4}$$

In the simulation study, we use the latter alternative, i.e., the spectrum width:

$$\Delta\alpha(q) \equiv \max_q \alpha(q) - \min_q \alpha(q) \tag{5}$$

as the measure of multifractality. Note that the results given by the singularity spectrum width and the generalized Hurst exponent width are qualitatively very similar, as shown in the recent study by Kukacka and Kristoufek (2020).

Table 1
Empirical example of multifractality.

| Asset | $\Delta\alpha(q)$ | mean ratio | confidence |
|--------------------|-------------------|------------|------------|
| 10Y Treasury Yield | 0.5002 | 2.8011 | 1.0000 |
| Apple Inc. | 0.2348 | 2.5849 | 1.0000 |
| Bitcoin | 0.7097 | 5.2475 | 1.0000 |
| Crude Oil | 0.2158 | 1.3740 | 0.7720 |
| EUR/USD | 0.1632 | 3.4157 | 0.9990 |
| Gold | 0.4478 | 5.8728 | 1.0000 |
| S&P500 | 0.2331 | 1.4844 | 0.8910 |

Note: $\Delta\alpha(q)$ is the estimated multifractal spectrum width for the given asset, *mean ratio* is the mean ratio between the estimated width and 1000 widths estimated on the resampled time series, and *confidence* represents the proportion of such ratios above 1.

2.2. Multifractal detrended fluctuation analysis

As an estimator of the generalized Hurst exponents that are in turn used to estimate the multifractal spectrum through $\Delta\alpha(q)$, we utilize the Multifractal Detrended Fluctuation Analysis (MF-DFA) that was proposed by Kantelhardt et al. (2002) as a generalization of the Detrended Fluctuation Analysis (DFA) of Peng et al. (1993) that has led to various other extensions (Podobnik and Stanley, 2008; Podobnik et al., 2011; Qian et al., 2015). The original DFA procedure builds on scaling of detrended variances of the integrated long-range dependent processes and estimates the Hurst exponent through a scaling law between the average variance estimated on subsamples of a given length and the length (scale) itself. For each scale s , the series is split into N_s nonoverlapping boxes and for each box ν , we calculate a mean squared error from a trend (usually linear) $F_{DFA}^2(\nu, s)$. Up to this point, the DFA and MF-DFA procedures are the same. The mean squared error is then averaged over all boxes of the same length s but with an exponential weight of $q/2$. For $q = 2$, i.e., the long-range dependence case, we obtain the standard average. The fluctuation function for scale s and moment q is given as:

$$F_q(s) = \left(\frac{1}{2N_s} \sum_{\nu=1}^{2N_s} (F_{DFA}^2(\nu, s))^{q/2} \right)^{1/q}. \tag{6}$$

We eventually obtain the generalized Hurst exponent $H(q)$ from the following scaling law:

$$F_q(s) \propto s^{H(q)}. \tag{7}$$

There are various specifications, mostly with respect to the type of detrending and scaling range. The details are given in Kantelhardt et al. (2002, p. 89–91). In our setting, we adhere to the linear detrending and set the minimal range to $s_{\min} = 10$ and the maximum range to $s_{\max} = T/10$ where T is the studied time series length. The step between scales is set to 10. There is no clear consensus on the minimum and maximum scales or steps between scales. We keep within the range of $s_{\min} = 5$ and $s_{\max} = T/4$ that are considered as extremes (compare Kantelhardt et al. (2001); Alvarez-Ramirez and Escarela-Perez (2010); Alvarez-Ramirez et al. (2010); Rak and Grech (2018)) and use the step between scales above 1 to keep the computational burden manageable. The range of moments is set between $q_{\min} = -4$ and $q_{\max} = 4$ with a step of $q_{\text{step}} = 1$. Similarly to the ranges of scales, there is no clear consensus on such ranges. Most frequently, these are set at $\pm 3, \pm 4, \pm 5$, or ± 10 . However, in the context of financial series, we stay conservative and opt for ± 4 as one might get to troubles with the existence of moments (Buonocore et al., 2017; Morales et al., 2012). As the generalized Hurst exponent is monotonous in moments q , one may measure multifractality only using the exponents for the lowest and highest moments. As a precaution for finite samples, we still estimate the generalized Hurst exponents and thus also the width of the spectra on a range of moments with a step of 1. Even though it is more common to use the step of 0.1 in many studies, it is purely for graphical purposes that we are not interested in.

Multifractality is often considered a measure of complexity of the underlying time series (Ivanov et al., 2001; Shimizu et al., 2002; Lopes and Betrouni, 2009). However, apart from correlations, being linear and mostly nonlinear, multifractality is also detected in processes with heavy tails (Jiang et al., 2019; Jiang and Zhou, 2008; Liu et al., 2008; Rak and Grech, 2018). Therefore, to distinguish between the types of apparent multifractality, we examine properties of the original simulated series as well as the shuffled series, where all correlations are removed by shuffling but the distributional properties remain. One is then able to separate these two sources. For illustration, Table 1 summarizes the estimated multifractal spectrum widths $\Delta\alpha(q)$ of daily logarithmic returns of different financial assets (a government bond, a stock, a cryptoasset, two commodities, an exchange rate, and a stock index) between 1 Jan 2014 and 30 Jun 2021. As statistical inference for multifractality measures is practically problematic to obtain analytically due to specific behavior under various distributional properties, correlation structures, and small/finite samples (Jiang et al., 2019), we present a mean ratio of estimated $\Delta\alpha(q)$ of the given series and its shuffled counterparts (1,000 random draws with replacement) to control for distributional and sample size effects. If there is no correlations-induced multifractality present in the data, the ratio is expected to be equal

to 1. We add a confidence measure that represents a proportion of ratios above 1. The highest ratios are found for gold and bitcoin pointing at the most complex dynamics in the data-generating processes. Five out of seven series show high mean ratios and confidence of 1 or very close to it. Crude oil seems to be the least complex of the list with the mean ratio close to 1 and a rather low confidence. A similar approach towards statistical inference is applied in the Monte Carlo simulation study that now follows.

3. Monte Carlo simulation study

3.1. General Monte Carlo setup

A unified setup of the Monte Carlo numerical studies for each model is described below. All computations are executed using R. To manage the computationally extensive Monte Carlo setup, we utilize parallel server capacities and take advantage of `doParallel` and the `foreach` packages. This combination enables an evaluation of independent for-loop iterations in parallel on multicore computational servers.

1000 independent runs ensure the statistical validity of the presented results for each experiment. Model output time series have a unified length $T = 20000$ after discarding 1000 initial burn-in observations so that a potential influence of the initial conditions is eliminated. Since we study models intended to simulate daily financial time series, the unified length $T = 20000$ is selected concerning the approximate maximum of the standardly available history of the US shares since the 1950s. [Fig. A.10](#) displays typical individual time series outputs of the examined models under this setup. While the left half of the figure is based on $T = 20000$, the right half zooms the respective left-hand side series for the 2000 middle observations to allow for a more detailed visual examination. The sufficiency of the initial burn-in period is assumed because we work with time series models of generally unpredictable financial returns. It is further supported by the visually stable dynamics of the depicted time series. [Table A.3](#) then complements the typical graphical outputs by aggregate descriptive statistics and their 90% sample confidence intervals based on 1000 random runs under the benchmark parameterization and the above-mentioned general simulation setup. We observe that even though the dynamics can be quite heterogeneous, there are no degenerate time series.

3.2. Design of the simulation study

For each financial agent-based model, we select its key parameters governing the model dynamics. Examples of these key parameters are, e.g., the intensity of choice governing the switching between trading strategies in the [Brock and Hommes \(1998\)](#), [Gauernsdorfer and Hommes \(2007\)](#), and [Schmitt \(2020\)](#) models, herding behavior intensities in the [Gilli and Winker \(2003\)](#) and [Alfarano et al. \(2005, 2008\)](#) models, parameters associated with the population dynamics of fundamentalists and chartists in the cusp catastrophe model, or the price misalignment parameter in the [Franke and Westerhoff \(2011\)](#) model, etc. We also propose a benchmark parameterization that always follows, where possible, the original research paper introducing the model or a most suitable follow-up research article proposing a specific model setup. The details for each model are presented in [Section 4](#).

As we aim to focus only on a few key parameters for each model, a simple and intuitive 2D grid search design represents a suitable methodology for our analysis. If one wanted to analyze multiple parameters in various combinations, the curse of dimensionality associated with this straightforward experimental approach would perhaps quickly exhaust any available computational resources and threaten to make the analysis infeasible, at least for the given extent of nine examined models. In [Section 6.5](#), we thus outline potential avenues for future research that could tackle this issue and enhance the potential for an additional more extensive analysis based on, e.g., a surrogate modeling method.

For selected pairs of parameters, we thus define a grid of parameterization setups by multiplying each benchmark parameter value by the factors of 1.25^i , $i \in \{-5, -4, -3, -2, -1, 0, 1, 2, 3, 4, 5\}$. Hence, we obtain a rich 11 rows \times 11 columns grid lattice of parameter combinations in which the benchmark parameterization appears at the middle [6, 6] position. Thus, the selected grid covers an approximate range between one-third and triple of the benchmark parameter values, allowing studying the models' behavior in their neighborhood in reasonable detail. The other parameters keep their benchmark values. If not explicitly stated otherwise, this setup is implemented by default with no modifications. Exceptional adjustments are always emphasized in the model description. An example in which we cannot utilize the general setup is, e.g., the specification of the grid of values for a memory parameter in the [Brock and Hommes \(1998\)](#) model that is already set to its theoretical borderline value within the benchmark parameterization.

For all 121 parameter combinations, we always compare the output for the original simulated series with the output for a randomly shuffled series. Shuffling the original series by randomly mixing all its observations results in eliminating any autocorrelation links. Therefore, this comparison serves as a tool to distinguish multifractality due to a complex agent-based correlation structure of the given model from multifractality due to distributional properties, mostly heavy tails, of the underlying data generating process.

3.3. Detection of multifractality due to an agent-based correlation structure

We always present two main figures with results in the format of an 11×11 ‘heat map’ lattice for each pair of parameters. The first one depicts the ‘multifractality strength.’ It displays the sample average of ratios between the multifractal spectra $\Delta\alpha(q)$ (5) for the original simulated series and the randomly shuffled series over all individual random runs. Simply put, based on a bootstrap, we first calculate the ratios, and subsequently, we evaluate the mean of its Monte Carlo distribution:

$$\text{multifractality strength}(q) = \frac{1}{N} \sum_{n=1}^N \frac{\Delta\alpha_{n,\text{original}}(q)}{\Delta\alpha_{n,\text{shuffled}}(q)}, \tag{8}$$

where typically $N = 1000$ random runs according to Section 3.1. The displayed color in the heat map gradually changes from red (dark) to pale as this ‘average multifractality ratio’ increases.

The second heat map depicts the sample-based confidence level that the multifractality strength (8) is higher than 1. More specifically, it displays the fraction of individual ratios higher than 1 over all random runs:

$$\text{confidence level for multifractality}(q) = \frac{1}{N} \sum_{n=1}^N I(n, q), \tag{9}$$

where an indicator function $I(n, q) = 1$ if $\frac{\Delta\alpha_{n,\text{original}}(q)}{\Delta\alpha_{n,\text{shuffled}}(q)} > 1$ and zero otherwise.

Together, these two figures indicate the presence of a statistically significant multifractality at the 5% level if the multifractality strength (8) is > 1 and the confidence level for multifractality (9) is ≥ 0.95 for a given parameter combination. The observed multifractality is then apparently driven by a complex agent-based structure of the model as in the randomly shuffled series considered in the denominator of the individual multifractality ratios, any autocorrelation dependence completely deteriorates. Moreover, we only present results for parameter combinations leading to at least 95% numerical stability of the simulated model over all random runs, ensuring that only non-diverging model setups are considered.

To elaborate the statistical significance of the multifractality even more thoroughly, we also present a third heat map with the confidence levels that a given multifractality strength ratio is statistically significantly different from the one associated with the benchmark parameterization. This statistical hypothesis is evaluated via the standard Welch’s unequal variances t -test (Welch, 1947) with the null hypothesis of equal means because the sample variances of the Monte Carlo distributions of the multifractality ratios based on 1000 random runs differ markedly across the grid:

$$\text{confidence level for differences} = 1 - p\text{-value of the Welch’s } t\text{-test}. \tag{10}$$

For a clear illustration, we depict this third type of the heat map also in the main text for the cusp and Ising models in Fig. 1 and Fig. 2, panel (c), but for the matter of space, for other models, we relegate it to Appendix, Fig. B.11. Naturally, each benchmark parameterization must be accompanied by the confidence level 0 (the darkest red), which also serves as a practical check of the graphical accuracy of the results. We kindly refer the reader to the GitHub repository for technical details of implementation and graphical depiction of the heat maps.

As a specific example, we can conclude that a model under the benchmark parameterization, usually depicted at the middle [6, 6] position of the heat map lattice, generates considerable multifractal patterns due to a complex agent-based correlation structure if we observe the multifractality strength noticeably higher than 1 in the first heat map, and the second heat map confirms its statistical confidence $\geq 95\%$. The third heat map then summarizes how statically significantly is the multifractality strength affected by the changes in model parameterization. And of course, the higher the multifractality strength and the respective confidence levels, the stronger multifractal pattern is detected.

4. Model ‘families’

All financial agent-based models analyzed in this paper have already been studied w.r.t. their general multifractal properties in a companion paper by Kukacka and Kristoufek (2020) where one can find complete formal descriptions of individual models together with complete benchmark parameterizations. We thus only focus on the key formulas containing selected parameters instead of the overall model descriptions for the current analysis. We also keep the formalism of model descriptions to avoid confusion. We especially aim at explaining the role that the analyzed parameters play in the model derivation or the impact they have on the overall model dynamics.

The following sections structure the nine models according to their ‘lineage’ to four model ‘families’ to foster discussion regarding various agent-based mechanisms and key model parameters. Table 2 summarizes all presented models with their main features and key references.

4.1. Oldest models inspired by other scientific disciplines

As modern Finance is a rather young scientific discipline, it is not surprising that the first financial agent-based models were inspired by other scientific disciplines. Namely, Biology in the case of the cusp catastrophe model, which was developed to explain sudden, discontinuous changes within morphogenetic processes, and Physics for the Ising model, which is clearly inspired by the model of ferromagnetism.

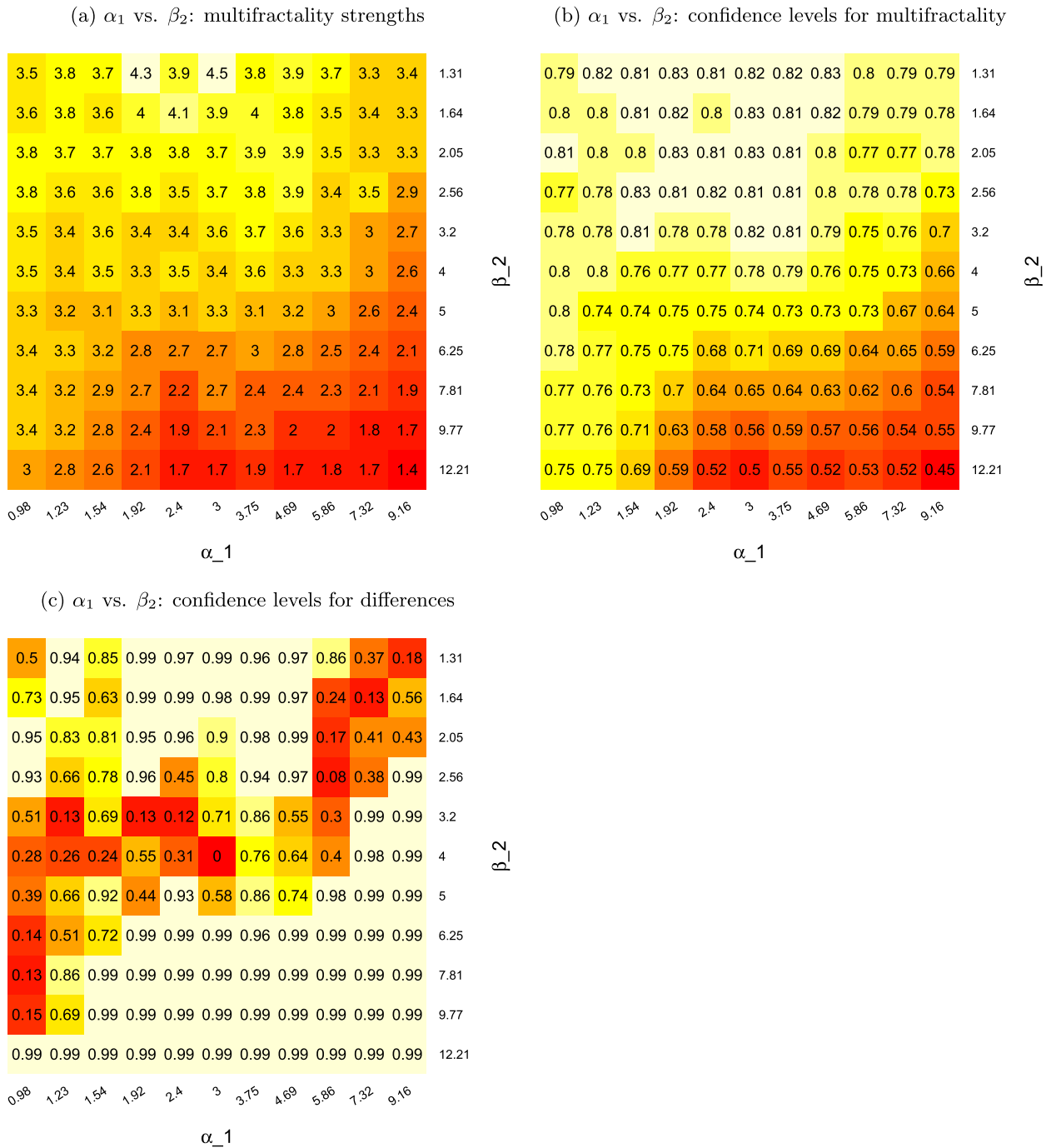


Fig. 1. Results for the cusp catastrophe model (1974) Note: The heat map color gradually changes from red (dark) to pale as the displayed value increases. The multifractality strength > 1 and the confidence level for multifractality ≥ 0.95 indicate the presence of a statistically significant multifractality due to a complex agent-based correlation structure at the 5% level. Similarly, values in panel (c) ≥ 0.95 indicate a statistically significant difference of the given ratio in panel (a) compared to the benchmark parametrization. The presented values are based on 1000 random runs and rounded to one and two decimal digits. The confidence level 0.99 stands for ≥ 0.99 . Depicted parameters: α_1 ...interacts with the 'fundamental' side of the market; β_2 ...interacts with the 'speculative' side of the market. (For interpretation of the references to colour in this figure legend, the reader is referred to the web version of this article.)

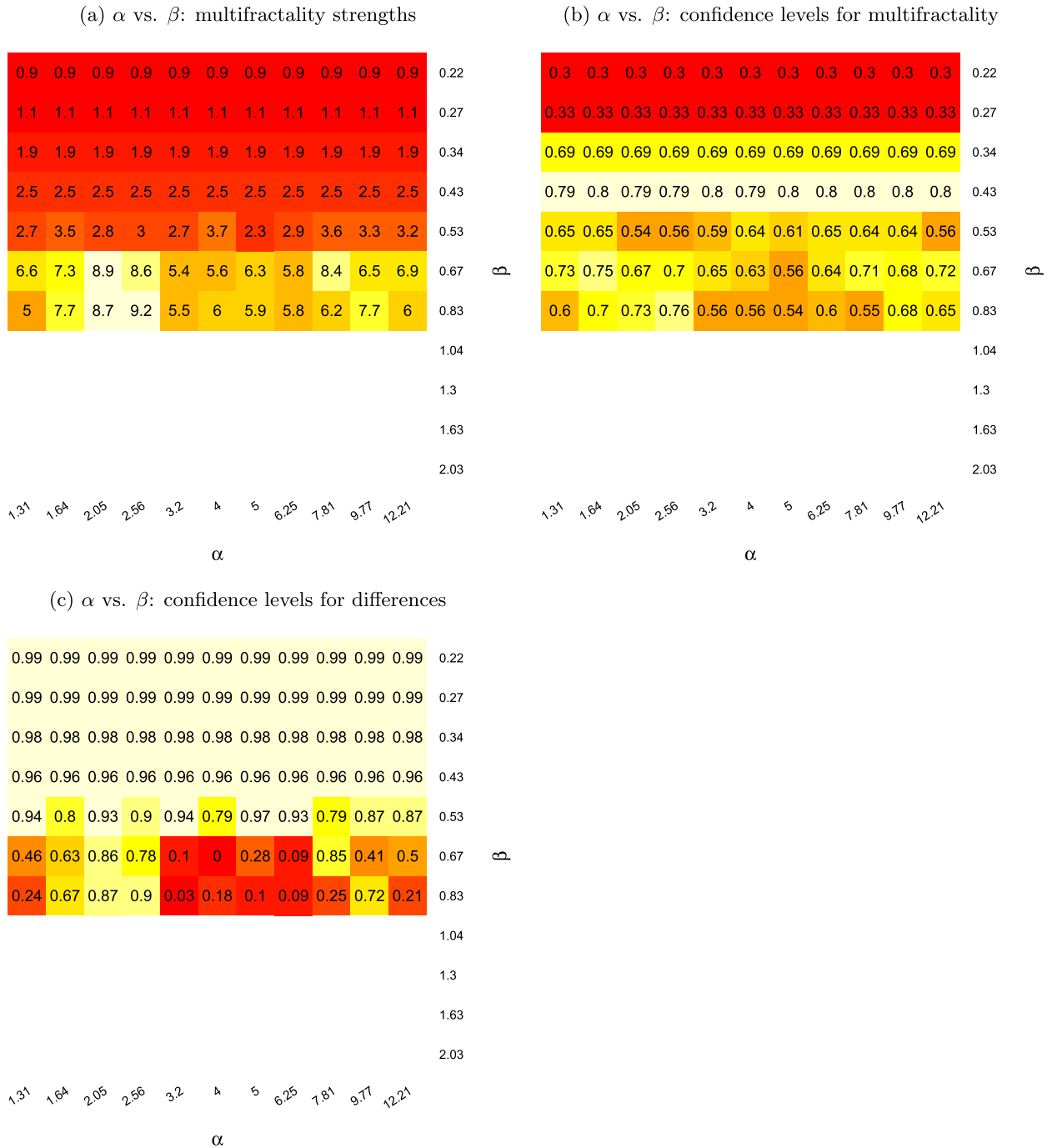


Fig. 2. Results for the Bornholdt (2001) Ising model Note: The heat map color gradually changes from red (dark) to pale as the displayed value increases. The multifractality strength > 1 and the confidence level for multifractality ≥ 0.95 indicate the presence of a statistically significant multifractality due to a complex agent-based correlation structure at the 5% level. Similarly, values in panel (c) ≥ 0.95 indicate a statistically significant difference of the given ratio in panel (a) compared to the benchmark parametrization. The presented values are based on 100 random runs and rounded to one and two decimal digits. The confidence level 0.99 stands for ≥ 0.99 . Depicted parameters: α ...global coupling parameter; β ...responsiveness parameter of the orientation updating of spins. (For interpretation of the references to colour in this figure legend, the reader is referred to the web version of this article.)

4.1.1. Cusp catastrophe model (1974)

Catastrophe Theory was proposed by Thom (1975) and one of the simplest deterministic model specifications, the cusp catastrophe, was suggested by Zeeman (1974) to model sudden crashes of stock markets as endogenous events triggered by trading activities of speculators. The model was extended to a stochastic version in Cobb (1981) by implementing a Gaussian white noise process to the derivation of the dynamic system. Barunik and Kukacka (2015) further develop a method that

Table 2
Models' presentation.

| Model | Key reference | Origin | Objective | Output | Types of agents | # of agents | Switching mechanism |
|--|---|----------|------------|--------------------------|------------------------|-------------------|--------------------------|
| Oldest models inspired by other scientific disciplines | | | | | | | |
| Cusp catastrophe | Zeeman (1974) | Biology | stocks | log-returns ^a | F&C | NA | continuous |
| Ising | Bornholdt (2001) | Physics | stocks, FX | log-returns | buyers & sellers | 1024 | ferromagnetism |
| Adaptive belief system family | | | | | | | |
| BH (1998) | Brock and Hommes (1998) | ABS | stocks | deviations ^b | F&C | unit population | multinomial logistic |
| GH (2007) | Gauernsdorfer and Hommes (2007) | ABS | stocks | returns | naive ^c F&C | unit population | binomial logistic |
| 'Ant' herding dynamics family | | | | | | | |
| GW (2003) | Gilli and Winker (2003) | ANT | FX | price ⇒ %Δ | F&C | 100 | transition probabilities |
| ALW (2005) | Alfarano et al. (2005) | IAH | stocks, FX | log-returns | F&noise traders | unit population | transition probabilities |
| ALW (2008) | Alfarano et al. (2008) | IAH | stocks, FX | log-returns | F&noise traders | 100 noise traders | sentiment index |
| Structural stochastic volatility family | | | | | | | |
| FW (2011) | Franke and Westerhoff (2011) | IAH | stocks, FX | log-returns | F&C | majority index | transition probabilities |
| SW (2017) | Schmitt and Westerhoff (2017) | IAH, ABS | stocks, FX | log-returns | F&C | unit population | binomial logistic |

Note: 'Origin' according to [Chen et al. \(2012\)](#): ABS stands for the adaptive belief system, ANT for the 'ant' type of system, and IAH for the interactive agent hypothesis. The main 'Objective' shows the type of market being primarily modeled. 'Output' reports the type of the generated time series. 'Types of agents' stands for the kind of involved agents (F&C...fundamentalists and chartists), and the '# of agents' displays their number under the benchmark parametrization (NA...not applicable). Finally, 'Switching mechanism' reports the mechanism used for dynamic updating of agents' market fractions, where applicable.

^avolatility-adjusted

^bfrom the constant fundamental price

^cso-called Efficient Market Hypothesis believers using a naive forecasting rule

allows for a rigorously correct application of the cusp in modeling turbulent stock market periods accompanied by strongly dynamic clustered volatility of stock returns. The solution is based on normalization of the stock market returns by their consistently estimated volatility utilizing the concept of realized variance.

The model simulates the time-variant equilibrium surface of the stochastic cusp catastrophe potential function as:

$$dy_t = (\alpha_{z,t} + \beta_{z,t}y_t - y_t^3)dt + dW_{1,t}, \tag{11}$$

where $\alpha_{z,t}$ and $\beta_{z,t}$ are the control variables representing the equilibrium state of the system and $W_{1,t}$ is the standard Wiener process. $\alpha_{z,t}$ and $\beta_{z,t}$ further linearly depend on n independent variables $z_{i,t}$, $i = 1 \dots, n$, $t = 1 \dots, T$, as follows:

$$\begin{cases} \alpha_{z,t} = \alpha_0 + \sum_{i=1}^n \alpha_i z_{i,t}, \\ \beta_{z,t} = \beta_0 + \sum_{i=1}^n \beta_i z_{i,t}. \end{cases} \tag{12}$$

Most importantly, the dimensions of the control space $\alpha_{z,t}$ and $\beta_{z,t}$ represent the asymmetry and the bifurcation sides of the model. The former is better known in the economic agent-based literature under the term 'fundamental' and the latter as 'speculative' sides of the market.

Benchmark The baseline parameterization follows [Barunik and Kukacka \(2015\)](#): the number of independent variables is set to $n = 2$ and their realizations are drawn from the uniform distribution $U(0, 1)$. Coefficients of (12) are set as: $\alpha_j = \{-2, 3, 0\}$ and $\beta_j = \{-1, 0, 4\}$, $j = \{0, 1, 2\}$.

Key parameters The setup ensures that $z_{1,t}$ solely determines the fundamental $\alpha_{z,t}$ side of the market since $\alpha_2 = 0$; and $z_{2,t}$ only drives the speculative $\beta_{z,t}$ side since $\beta_1 = 0$. In a trivialized real-world parable, we can think of $z_{1,t}$ as a variable representing fundamental investors, e.g., large institutional funds, while the variable $z_{2,t}$ substitutes for speculative money in the market and trading activities of so-called chartists. Parameters governing the model dynamics are therefore α_1 and β_2 that interact with the 'fundamental' variable $z_{1,t}$ or the 'speculative' $z_{2,t}$, respectively. Increasing α_1 thus strengthens the stabilizing role of the fundamental traders during the bullish and bearish phases of the market, i.e., before and after the crash, in which they exert the reverting pressure since they perceive the market overvalued or undervalued, respectively. Increasing β_2 , on the other hand, supports the destabilizing forces by the speculators leading the market to the bifurcation region where speculators are leaving the market 'en masse', which may trigger a stock market crash.

4.1.2. Bornholdt (2001) Ising model

The [Bornholdt \(2001\)](#) financial market version of the Ising model parallelizes an asset market to the ferromagnetic model. Buyers are represented by spins with a positive (+1) and sellers with a negative (-1) value located in an $L \times L$ squared lattice. The values of spins are dynamically updated in time so that the j th spin $S_{j,t+1}$, $j = 1 \dots, L^2$, $t = 1 \dots, T$ represents a buyer with a probability $P_{i,t} = 1/(1 + \exp(-2\beta h_{i,t}))$, where β is a responsiveness parameter, and a seller with the complementary probability. The local field $h_{i,t}$:

$$h_{i,t} = \sum_{j=1}^{L^2} J_{i,j} S_{j,t} - \alpha C_{i,t} \left| \frac{1}{L^2} \sum_{j=1}^{L^2} S_{j,t} \right|, \tag{13}$$

combines the neighboring forces, where $J_{i,j} = 1$ for the four nearest neighbors and zero otherwise, and the reaction to the global prices, where $\alpha > 0$ is a global coupling parameter and $C_{i,t}$ represents a strategy of spin i .

Interestingly, [Cont and Bouchaud \(2000\)](#) suggest a related model also based on the original Ising framework that is able to explain the relations between the observed heavy tails in the financial data and the herding behavior of investors.

Benchmark The baseline parameterization follows [Kristoufek and Vosvrda \(2018\)](#) who set $\alpha = 4$, $\beta = 2/3$, and $L = 32$. Due to an enormous computational burden of the model algorithm, we present results based on 100 independent runs of the simulation experiment instead of the usual 1000 runs.

Key parameters We study the combinations of the global coupling parameter α reflecting the strength of the minority game behavior and the responsiveness parameter of the orientation updating of the individual spins β .

4.2. Adaptive belief system family

The evolutionary switching principle based on the bi/multinomial logistic model originally introduced by [Brock and Hommes \(1997\)](#) became widely applied in the financial agent-based literature. Its financial market application leads to a stylized adaptive endogenous selection among a ‘menu’ of different trading strategies. The dynamics of this feedback system thus depend not only on the model observables and random shocks but is predominantly driven endogenously by the future heterogeneous expectations ([Lucas, 1978](#)) of the market participants.

4.2.1. Brock and Hommes (1998) heterogeneous agent model

In the famous [Brock and Hommes \(1998\)](#) model, the population of investors is provided with a heterogeneous set of trading strategies, among which they choose based on the observed past profitability. [Hommes \(2006\)](#) suggests a compact notation of the system of equations that we further condense to:

$$Ry_t = \sum_{h=1}^H x_{h,t-1} (g_h y_{t-1} + b_h) + \varepsilon_t, \tag{14}$$

$$x_{h,t-1} = \frac{\exp(\gamma[U_{h,t-1} + \delta U_{M,h,t-2}])}{\sum_{h=1}^H \exp(\gamma[U_{h,t-1} + \delta U_{M,h,t-2}])}, \tag{15}$$

where (14) represents a pricing formula determining the price level of a risky asset $p_t = y_t + \bar{p}$, $t = 1 \dots, T$, in which \bar{p} is the fundamental price, R is the risk-free gross interest rate, and ε_t is an independent and identically distributed (i.i.d.) error term. Most importantly, $x_{h,t-1}$ are the population fractions of investors following the ‘h-type’ $h \in \{1, \dots, H\}$ trading strategy $g_h y_{t-1} + b_h$ defined by a trend parameter g_h and a bias parameter b_h . While the fundamental trading strategy suggests $g_h = b_h = 0$, different technical trading strategies and extrapolation techniques used by chartists can be defined via various combinations of a nonzero trend and bias parameters. (15) defines the population fraction $x_{h,t-1}$ of investors using the trading strategy h applying the multinomial logit formula. Here, $U_{h,t-1}$ is the h^{th} recently observed profitability, $U_{M,h,t-2}$ is its historically observed past probability determined by the ‘memory’ parameter $0 \leq \delta \leq 1$, and $\gamma \geq 0$ is the intensity of choice.

Benchmark The baseline parameterization follows the setup suggested in [Kukacka and Barunik \(2013, 2017\)](#) and [Polach and Kukacka \(2019\)](#): $R = 1.0001$, $\varepsilon_t \sim N(0, 0.1)$, $H = 2$, $g_1 = b_1 = 0$, $g_2 = 0.4$, $b_2 = 0.3$, $\gamma = 10$. Finally, the memory parameter is set to $\delta = 0.99$ ([Gauersdorfer and Hommes, 2007](#)).

Key parameters Parameters governing the model dynamics comprise the specification of the switching formula (15): the intensity of choice γ and the memory δ ; and the trend and bias parameters from (14): g_h and b_h , respectively. W.r.t. the former pair, γ determines the willingness of investors to switch between the trading strategies based on their past profitability. Extreme theoretical values suggest the following behavior. For $\gamma = 0$, there is no switching among trading strategies; for $\gamma = +\infty$, all investors switch to the currently most profitable strategy during each period. For $0 \leq \gamma \leq +\infty$, some investors keep the ‘status quo’ but some switch to a more attractive strategy each period. Parameter δ represents the strength of the memory of investors since it actually dilutes the perception of the past realized profitability via a weighted average formula. Finally, the trend and bias parameters set as $g_2 > 0$ and $b_2 > 0$ represent a trend-following strategy that is slightly upward-biased, the combination that most likely corresponds to the average aggregate behavior of the speculative side of the stock markets ([Kukacka and Barunik, 2017](#)).

Importantly, the general design of the simulation study ([Section 3.2](#)) needs to be partially adjusted for this model. For δ , we set up the grid range using discrete steps applied by subtracting $0.004 \times j$, $j \in \{8, 7, 6, 5, 4, 3, 2, 1, 0, -1, -2\}$ from the benchmark value since $\delta = 0.99$ is already very close to its theoretical border 1. This leads to the location of the benchmark parameterization at the [9, 6] position of the 11×11 grid lattice instead of the middle position for panels (a) and (b) in [Fig. 3](#). For other parameters, we apply the general simulation setups. The benchmark parameterization for panels (c) and (d) thus keeps the middle [6, 6] position.

4.2.2. Gauersdorfer and Hommes (2007) model for volatility clustering

[Gauersdorfer and Hommes \(2007\)](#) propose an adaptation of the [Brock and Hommes \(1998\)](#) framework and enrich the original model in several aspects. This modification, while rather minor from the theoretical viewpoint, markedly improves the model ability to replicate empirically observed clustering of volatility. The expectation formation mechanism no longer

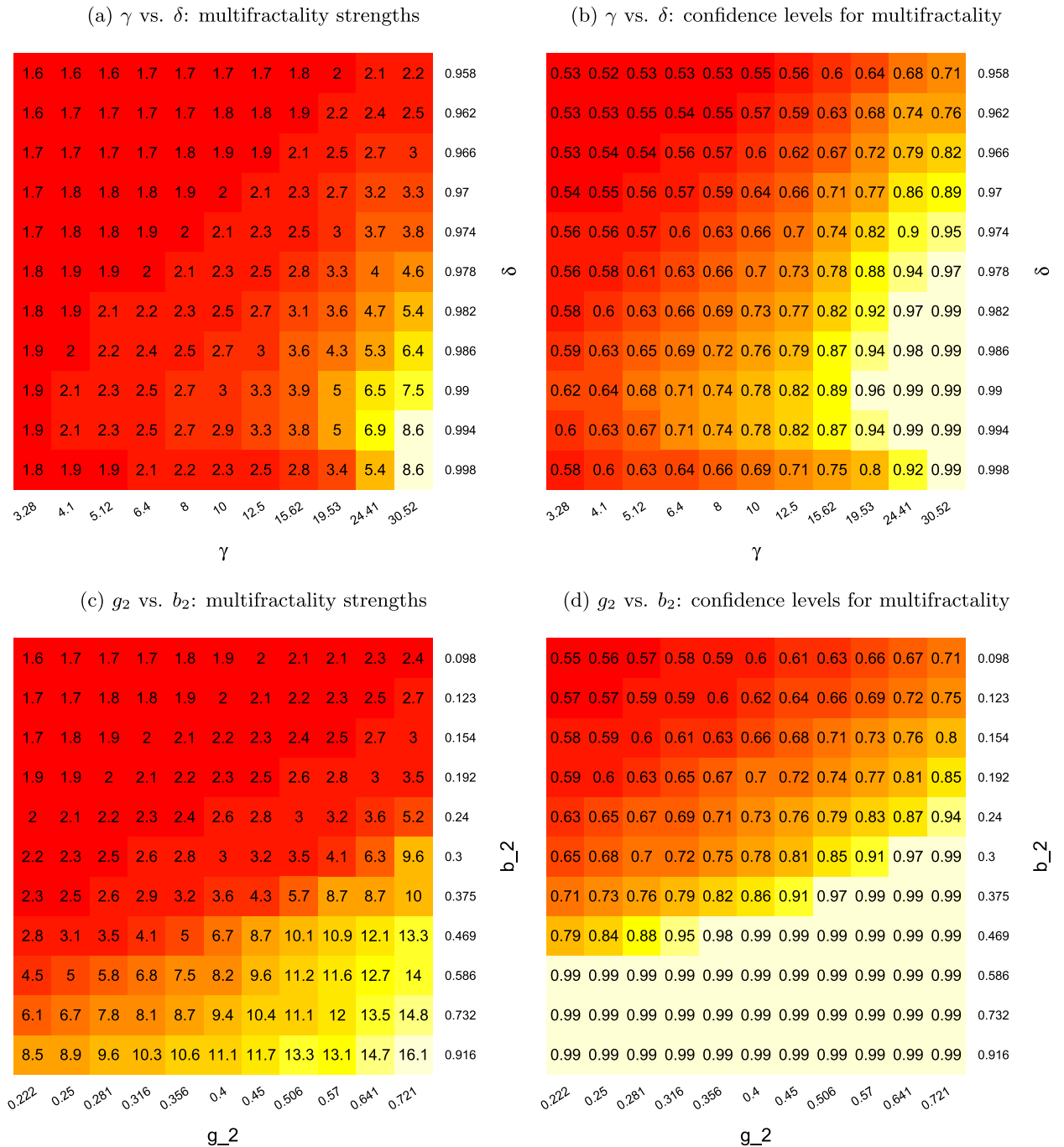


Fig. 3. Results for the Brock and Hommes (1998) model Note: The heat map color gradually changes from red (dark) to pale as the displayed value increases. The multifractality strength > 1 and the confidence level for multifractality ≥ 0.95 indicate the presence of a statistically significant multifractality due to a complex agent-based correlation structure at the 5% level. The presented values are based on 1000 random runs and rounded to one and two decimal digits. The confidence level 0.99 stands for ≥ 0.99 . Depicted parameters: γ ...intensity of choice; δ ...memory; g_2 ...trend extrapolation; b_2 ...bias. The benchmark parameterization in (a) and (b) exceptionally appears at the [9, 6] position. (For interpretation of the references to colour in this figure legend, the reader is referred to the web version of this article.)

follows the general specification of an 'h-type' trading strategy in (14), but, for $H = 2$, the fundamentalists' (f) and chartists' (c) expectations are set as:

$$\begin{cases} E_{f,t-1}[p_t] = \bar{p} + v(p_{t-2} - \bar{p}), \\ E_{c,t-1}[p_t] = p_{t-2} + w(p_{t-2} - p_{t-3}), \end{cases} \tag{16}$$

where p_t is a price level of a risky asset, $t = 1 \dots, T$, \bar{p} is the fundamental price, $0 \leq \nu \leq 1$ is the fundamentalists' parameter, and $w \geq 0$ is the trend-following parameter for chartists.

The switching dynamics of population fractions follow (15) in the first step, but the additional step introduces a 'penalty' to the fraction of chartists based on an actual distance between the current price level and \bar{p} :

$$\begin{cases} \tilde{x}_{c,t-1} = x_{c,t-1} \exp[-(p_{t-2} - \bar{p})^2 / \psi], \\ \tilde{x}_{f,t-1} = 1 - \tilde{x}_{c,t-1}, \end{cases} \tag{17}$$

where $\psi > 0$ is the correction term. When the price deviates markedly from its fundamental value, the exponential correction in the denominator increases and effectively decreases the population fraction of chartists compared to a standard result of (15). The unchanged result of the binomial switching formula (15) only applies for $p_{t-2} = \bar{p}$.

Benchmark The baseline parameterization follows Gaunersdorfer and Hommes (2007) and Gaunersdorfer et al. (2008): $H = 2$, $\nu = 1$, $w = 1.9$, the fundamental price $\bar{p} = 1000$, and the correction term $\psi = 1800$. The intensity of choice and the memory parameter in (15) are set as: $\gamma = 2$, $\delta = 0.99$.

Key parameters We first study the combination of parameters of the two elementary trading strategies, ν and w . The benchmark setup of $\nu = 1$, essentially a naive forecast, already represents a 'pure' version of the fundamental behavior consistent with the Efficient Market Hypothesis. Second, we focus on the combination of the intensity of choice γ (see Section 4.2.1 for a discussion of its impact on the model dynamics) and the correction term ψ that reflects worries of chartists from a growing probability of a forthcoming correction due to an increasing deviation between the current and fundamental price. This parameter can be understood as a penalty due to a growing mispricing since it effectively hinders the evolution of large price deviations based on the extrapolative trend-following behavior. It thus serves as a stabilizing term of the system.

The general design of the simulation study (Section 3.2) again needs to be partially adjusted. For ν , we set up the grid range using discrete steps applied by subtracting $0.01 \times j$, $j \in \{10, 9, 8, 7, 6, 5, 4, 3, 2, 1, 0\}$ from the benchmark value because for $\nu > 1$, the model exhibits explosive behavior. This leads to the location of the benchmark parameterization at the [6, 11] position of the 11×11 grid lattice instead of the [6, 6] position for panels (a) and (b) in Fig. 4. For other parameters, we apply the general simulation setups. The benchmark parameterization for panels (c) and (d) thus keeps the middle [6, 6] position.

4.3. 'Ant' herding dynamics family

The third family of models follows the 'ant dynamics' tradition introduced by Kirman (1991, 1993). This interesting concept of herding behavior represents another frequently used principle of the dynamics of population fractions in financial agent-based models as it can trigger nonlinear endogenous dynamics leading to large fluctuations of the entire market. Based on direct interactions, agents of one sub-population can persuade and 'recruit' the members of another sub-population to join their group.

4.3.1. Gilli and Winker (2003) model of herding

Gilli and Winker (2003) computationally implement the Kirman (1991, 1993) model and link the herding behavior based on discrete interactions to the activities of FOREX market participants. Based on the notation in Barde (2016), there are N agents in the model divided to two subgroups: fundamentalists (f) and chartists (c). The dynamics of the model are governed by switching probabilities:

$$\begin{cases} P_t^{c \rightarrow f} = (1 - x_t)(\varepsilon + \rho x_t), \\ P_t^{f \rightarrow c} = x_t(\varepsilon + \rho(1 - x_t)), \end{cases} \tag{18}$$

where x_t represents the population fraction of fundamentalists in time t , $t = 1 \dots, T$, ε is the probability of a spontaneous switch between f and c groups, and ρ is the probability of a successful recruitment. Expectations about the price p_t of the two groups are then defined as:

$$\begin{cases} E^f(\Delta p_t) = \phi(\bar{p} - p_{t-1}), \\ E^c(\Delta p_t) = p_{t-1} - p_{t-2}, \end{cases} \tag{19}$$

where ϕ is the adjustment speed to the fundamental price \bar{p} .

Benchmark The baseline parameterization follows the original Gilli and Winker (2003) setup, where $N = 100$ agents, switching probabilities $\rho = 0.264$ and $\varepsilon = 0.0001$, the adjustment speed $\phi = 0.0225$, and the fundamental price $\bar{p} = 1000$.

Key parameters Naturally, we first focus on the probabilities of a spontaneous switching ε and of a successful recruitment ρ as the key drivers of the dynamics of the model. Increasing both probabilities is hypothesized to have an increasing impact on modeling complexity. Second, we also study the impact of the adjustment speed on the fundamental price ϕ and the number of individual traders in the model N , rounded to integer values. Increasing N can be generally expected to have a positive impact on the complexity of the model since a model populated by more agents can intuitively exhibit more complex behavior. The impact of the adjustment speed ϕ is kept without prior expectation.

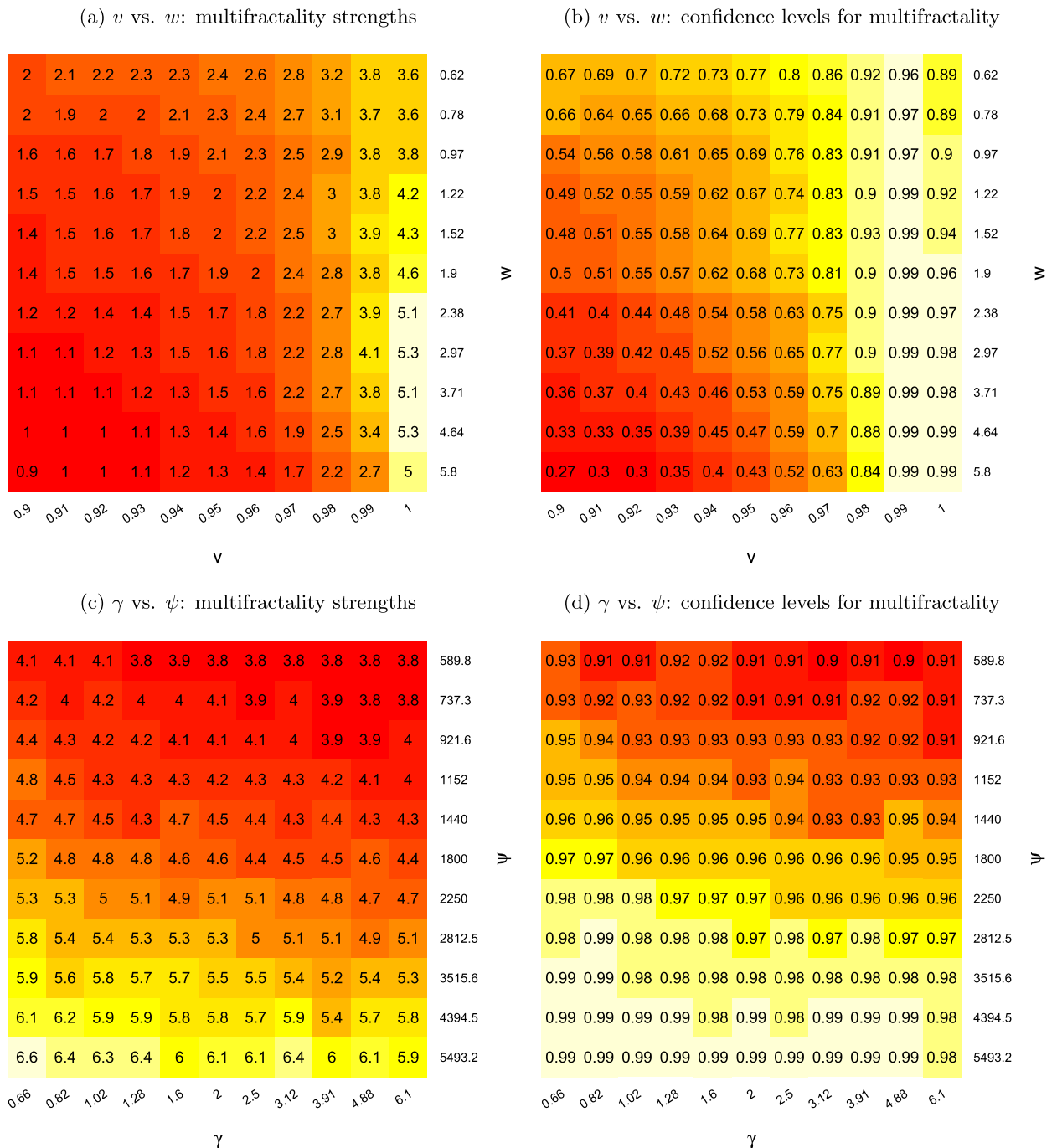


Fig. 4. Results for the Gaurersdorfer and Hommes (2007) model Note: The heat map color gradually changes from red (dark) to pale as the displayed value increases. The multifractality strength > 1 and the confidence level for multifractality ≥ 0.95 indicate the presence of a statistically significant multifractality due to a complex agent-based correlation structure at the 5% level. The presented values are based on 1000 random runs and rounded to one and two decimal digits. The confidence level 0.99 stands for ≥ 0.99 . Depicted parameters: v ...fundamentalists' parameter; w ...trend-following parameter for chartists; γ ...intensity of choice; ψ ...mispricing correction for trend followers. The benchmark parameterization in (a) and (b) exceptionally appears at the [6, 11] position. (For interpretation of the references to colour in this figure legend, the reader is referred to the web version of this article.)

4.3.2. Alfarano, Lux, and Wagner (2005) model of asymmetric herding

The model by Alfarano et al. (2005) generalizes the concept of the 'ant mechanics' by implementation of asymmetric herding tendencies. There are two subpopulations of N market participants consisting of n_t fundamentalists (f), who believe in price reversals to the fundamental value, and $N - n_t$ chartists (c), who are essentially noise-traders. The population

fractions dynamically update according to asymmetric switching probabilities:

$$\begin{cases} P_t^{c \rightarrow f} = (N - n_t)(\varepsilon_1 + n_t)\rho, \\ P_t^{f \rightarrow c} = n_t(\varepsilon_2 + (N - n_t))\rho, \end{cases} \tag{20}$$

where ε_1 and ε_2 are parameters governing asymmetric probabilities of a spontaneous switch from $c \rightarrow f$ or from $f \rightarrow c$, respectively, and ρ is a probability of a successful recruitment.

Benchmark The baseline parameterization follows [Alfarano et al. \(2005\)](#): $\varepsilon_1 = 16$, $\varepsilon_2 = 4.9$, and $\rho = 0.0025$. The number of market participants is not calibrated since an analytical solution for the model is derived for large N .

Key parameters There are three parameters of the model presumably influencing the complexity of the model. The parameters ε_1 and ε_2 have a positive impact on the switching probabilities of fundamentalists and chartists, respectively, so one might also expect them to be positively associated with the complexity of the model, which is a rationale partially based on the results of the [Gilli and Winker \(2003\)](#) model. On the other hand, since both parameters are solely associated with spontaneous switching and there is also a probability parameter of a successful recruitment ρ that represents the strength of the herding tendency of the model participants, one might preferably expect ρ to be positively associated with model complexity and keep the expectation about the impact of ε_1 and ε_2 undefined.

4.3.3. Alfarano, Lux, and Wagner (2008) model

The model by [Alfarano et al. \(2008\)](#) no longer implements asymmetric herding behavior of its predecessor ([Alfarano et al., 2005](#)). There is a subpopulation of fundamentalists and a subpopulation of n_c noise traders in the model. Noise traders are characterized by a dynamic switching process of opinion changes between an optimistic and a pessimistic mood that governs the overall herding dynamics of the model. The transition probabilities are determined by the Poisson intensity $a \geq 0$ of autonomous switching and the ‘herding-based’ pairwise switching rate $b \geq 0$. The case of $b > a$ is associated with an intensive herding that leads to strong majorities of optimistic or pessimistic noise traders. The model is then characterized by a bimodal distribution of the sentiment index $x_t \in \{-1, 1\}$:

$$dx_t = \frac{2n_{o,t}}{n_c} - 1 = -2ax_t dt + \sqrt{2b(1 - x_t^2) + \frac{4a}{n_c}} dB_{2,t}, \tag{21}$$

$$d\bar{p}_t = \sigma_f dB_{1,t}, \tag{22}$$

where $n_{o,t}$ represents the number of optimistic noise traders at time t , $t = 1 \dots, T$, $B_{1,t}$ and $B_{2,t}$ are independent Wiener processes, \bar{p}_t denotes the log fundamental price, and $\sigma_f \geq 0$ is the standard deviation of innovations to the fundamental price. The sentiment index $x_t = 0$ for a balanced sentiment and reaches positive or negative values for optimistic or pessimistic majorities of noise traders.

Benchmark The baseline parameterization follows [Ghonghadze and Lux \(2016\)](#) and [Chen and Lux \(2018\)](#) and their Langevin approximation of the model, where $n_c = 100$, $a = 0.0003$, $b = 0.0014$, and $\sigma_f = 0.03$.

Key parameters Naturally, the intensity $a \geq 0$ governing autonomous switches of opinion together with the rate $b \geq 0$ of ‘herding-based’ pairwise switching are the key parameters influencing the model dynamics and presumably also the model complexity. We hypothesize that both have a positive impact on the multifractal behavior of the model. Additionally, we study the impact of the standard deviation of fundamental innovations σ_f together with the number of noise traders n_c , rounded to integer values. Increasing the number of noise traders is expected to increase the complexity of the model, whereas for the magnitude of innovations, one can argue both ways: larger innovations are likely to support nonlinear dynamics of the model that might lead to higher complexity of the system, but, on the other hand, smaller innovations might make the system less stochastic, leading to higher predictability.

4.4. Structural stochastic volatility family

Other successors of the [Kirman \(1993\)](#) tradition of the ‘ant’ herding mechanism are [Franke and Westerhoff \(2011, 2016\)](#). However, the authors further emphasize the concept of structural stochastic volatility as an important source of complex dynamics supporting the financial stylized facts replication.

4.4.1. Franke and Westerhoff (2011) structural stochastic volatility model

In the [Franke and Westerhoff \(2011, 2016\)](#) model, there are N market participants in the model, n_t fundamentalists (f) and $N - n_t$ chartists (c). The majority index is defined as $x'_t \in \{-1, 1\} = (2n_t - N)/N$ and reaches its maximum for a market populated only by fundamentalists. Switching probabilities follow:

$$\begin{cases} P_t^{c \rightarrow f} = \nu \exp(s_t), \\ P_t^{f \rightarrow c} = \nu \exp(-s_t), \end{cases} \tag{23}$$

where ν represents a flexibility parameter and s_t is the switching index: $s_t = a_0 + a_x x'_{t-1} + a_d (p_{t-1} - \bar{p})^2$, where a_0 is an autonomous switching parameter, $a_x > 0$ is a herding parameter, $a_d > 0$ determines the influence of price misalignment, and \bar{p} is the log fundamental price.

The excess demand functions are defined as:

$$\begin{cases} d_t^f = \phi(\bar{p} - p_t) + u_t^f, \\ d_t^c = \chi(p_t - p_{t-1}) + u_t^c, \end{cases} \tag{24}$$

where ϕ and χ are adjustment parameters for fundamentalists and chartists, respectively, and i.i.d. $u_t^f \sim N(0, \sigma_f^2)$ and $u_t^c \sim N(0, \sigma_c^2)$ amend each of the excess demands with a group-specific stochastic noise.

Benchmark The baseline parameterization follows Franke and Westerhoff (2016): the flexibility parameter $\nu = 0.05$; $a_0 = -0.155$, $a_\chi = 1.299$, and $a_d = 12.648$; $\bar{p} = 0$; the excess demand parameters $\phi = 0.198$ and $\chi = 2.263$; $\sigma_f = 0.782$ and $\sigma_c = 1.851$.

Key parameters In the grid analysis, we first tune the price misalignment a_d and the flexibility parameter ν . As a_d in fact drives the mean-reversion tendency, i.e., decreases the propensity to switch and stabilizes the model, while increasing ν increases the switching probabilities, one might expect the model complexity to be negatively related to a_d and positively to ν . We further study the impact of the two adjustment parameters ϕ and χ . Because fundamentalists serve as a stabilizing force of the market while chartists destabilize the system, one might expect the model complexity to be positively related to ϕ and negatively to χ .

4.4.2. Schmitt and Westerhoff (2017) model with sunspots

The agent-based model by Schmitt and Westerhoff (2017) represents a simple large-scale framework that shares many common features with the Franke and Westerhoff (2011) model but also the binomial logistic switching mechanism with the Adaptive belief system family. While individual market participants are characterized by their own individual trading rules, under a set assumptions, e.g., a large number of agents, the large-scale model can be translated into a small-scale version. One of the main distinguishing innovations is that the stochastic errors for the individual trading rules are not independently distributed. Instead, they follow a multivariate-normal distribution with a time-varying covariance structure. In case of high mutual correlation, occasional ‘sunspot’ occurrences influence the model dynamics. The ‘sunspots’ represent various rare but crucial real-world financial market events, e.g., an unexpected exogenous shock with potential to trigger an extreme market episode or a strong short-term influence by opinion leaders.

We analyze the ‘S-CF’ model version, where sunspots can influence the behavior of both chartists and fundamentalists. There are N agents in the model and the time-varying variance-covariance matrices of the error distributions are characterized by elements $\rho^C = X^C/N$ and $\rho^F = X^F/N$, where X^C, X^F follow:

$$\begin{cases} X_{t-1}^C = \begin{cases} X^{C,h} \text{ with probability } S^C \\ X^{C,l} \text{ with probability } 1 - S^C, \end{cases} \\ X_{t-1}^F = \begin{cases} X^{F,h} \text{ with probability } S^F \\ X^{F,l} \text{ with probability } 1 - S^F, \end{cases} \end{cases} \tag{25}$$

where $X^{C,h}, X^{C,l}, X^{F,h}, X^{F,l}$ define the (l)ow and (h)igh boundaries, and S^C, S^F represent sunspot event probabilities for probabilities for chartists and fundamentalists, respectively. The market fraction of chartists follows:

$$W_{t-1}^C = \frac{1}{1 + \exp(\gamma[b^0 + b^H(1 - 2W_{t-2}^C) + b^M(F - P_{t-2})^2])}, \tag{26}$$

where γ is the intensity of choice, and b^0, b^H , and b^M represent the predisposition, herding, and price misalignment parameters, respectively. The parameters in (26) are homogeneous for the whole model population.

Benchmark The baseline parameterization follows Schmitt and Westerhoff (2017, Table 2, S-CF, Fig. 5): $X^{C,h} = 20$, $X^{F,h} = 40$, $S^C = 0.009$, $S^F = 0.005$; $\gamma = 1$, $b^0 = -0.336$, $b^H = 2.446$, $b^M = 19.671$.

Key parameters We first study the combination of the sunspot events probabilities S^C, S^F associated with the behavior of chartists and fundamentalists, respectively. Since sunspots represent completely unpredictable stochastic market events, one might hypothesize both probabilities to be negatively associated with model complexity. Based on experience with analysis of the Franke and Westerhoff (2011) model, we further study the impact of the price misalignment parameters b^M and the intensity of choice γ , which is not implemented in the Franke and Westerhoff (2011) model. As these two parameters appear in the denominator of (26), their increase tends to reduce the fraction of fundamentalists in the market.

5. Results and interpretation of the multifractal analysis

5.1. Oldest models inspired by other scientific disciplines

5.1.1. Cusp catastrophe model (1974)

Fig. 1 depicts the results for the cusp model. The middle [6, 6] positions of the heat map lattice with the benchmark parameterization suggest that while panel (a) displays an average ratio between the estimated multifractal spectrum $\Delta\alpha(q)$ for the original simulated series and the randomly shuffled series of 3.4, this ratio is significantly higher than 1 only at the 78% confidence level (panel b). That means it is not significantly higher than 1 even at the 20% level. Such a seemingly

contradictory behavior indicates that while the multifractality strength ratios based on some individual random runs of the model are very high, leading to an average of 3.4, however, only 78% of the runs lead to an individual ratio higher than 1. This result is naturally comparable with the conclusions of Kukacka and Kristoufek (2020) because the middle [6, 6] positions of the heat map lattice follow the identical benchmark parameterization.

More importantly, we observe a clear pattern of a potential multifractality evolution within the grid of parameter combinations. The multifractality strength due to the agent-based correlation structure of the cusp model slightly increases in the 'North-North-West' and the 'North-North-East' directions from the middle [6, 6] position, i.e., with decreasing the β_2 parameter, while significantly decreases in the 'South-East' direction, i.e., with increasing both key parameters. However, for any parameter combination, the multifractality remains clearly statistically insignificant at standard levels as captured in panel (b), although an increasing tendency of the confidence level follows the same direction as for the increasing multifractality strength.

Panel (c) then provides additional information about the statistical confidence of differences between the specific multifractality strength ratios vs. the benchmark middle [6, 6] position based on the Welch's unequal variances *t*-test. Although the individual multifractality measures remain statistically insignificant according to panel (b), the numerical differences among them gain even strong statistical significance following similar directions as for the above-commented increases and decreases of the multifractality strength.

To conclude, the multifractal sensitivity analysis extends the parameterization-specific results of Kukacka and Kristoufek (2020); however, it still does not suggest any considerable multifractal properties of the cusp catastrophe model even under a rich grid of proposed parameterizations of the key model parameters.

5.1.2. Bornholdt (2001) Ising model

Fig. 2 depicts the results for the Bornholdt (2001) Ising model. The benchmark [6, 6] positions reveal a considerable multifractality strength of 5.6 (panel a), which is, however, statistically significantly higher than 1 only at the 63% confidence level (panel b).

Most importantly, the global coupling parameter α does not seem to have any systematic impact on the complexity of the model. W.r.t. the responsiveness parameter β , its increasing value is associated with an increasing multifractality strength for lower β s reaching the highest values for and slightly above the benchmark parametrization. On the contrary, $\beta \geq 1.04$ and higher lead to a numerical divergence of the model. This is an expected outcome as the original Ising model has a critical temperature of a transition from a ferromagnet to a paramagnet that depends on β for a given α (Bornholdt, 2001). In the analyzed model, for high β , any positive/negative h then means 'buy'/'sell,' and the system quickly converges to the situation of zero returns, and it actually collapses. Such situations are represented by black positions in the grid of results.

We can observe the highest confidence levels of the multifractal properties under $\beta = 0.43$. This finding has a clear interpretation from the field of physics as for $\alpha = 0$ in the original Ising model, the critical temperature $1/\beta = 2.269 \Rightarrow \beta \doteq 0.44$. However, the confidence level that the multifractality strength is significantly higher than 1 never exceeds 80% (panel b) irrespective of the value of α .

Finally, the statistical significance of multifractality differences w.r.t the benchmark middle [6, 6] position reported in panel (c) suggests a rather clear pattern: multifractality strengths are generally not statistically significantly different at the 5% level in the close neighborhood of the benchmark parameterization, but again, under already highlighted $\beta = 0.43$ and lower, their differences gain increasing statistical significance.

To conclude, our analysis mainly supports the setup of the responsiveness parameter β around the benchmark value, which produces one of the strongest multifractal behaviors. In contrast, the global coupling parameter α does not exhibit any systematic impact. However, the level of multifractality driven by a complex agent-based correlation structure of the model is statistically insignificant for any combination of these two key parameters.

5.2. Adaptive belief system family

5.2.1. Brock and Hommes (1998) heterogeneous agent model

Fig. 3, panels (a) and (b), depict the results for the intensity of choice γ and the memory δ . The benchmark [9, 6] positions suggest a considerable multifractality strength of 3.0 (panel a), which is, however, statistically higher than 1 only at the 78% confidence level (panel b). Nonetheless, we can observe a pattern of further multifractality evolution. The multifractality due to the agent-based correlation structure markedly increases in the 'South-East-East' and the 'North-East-East' directions from the benchmark [9, 5] positions, i.e., with increasing γ even keeping δ fixed or with increasing both. It also gains statistical confidence in the same direction: already for the circa doubled $\gamma = 19.53$, even when benchmark δ is fixed, we observe a strongly statistically significant multifractality driven by a complex agent-based structure of the model represented by the average multifractality ratio (panel a) of 5.0 and the 96% confidence level. In contrast, combinations in other directions from [9, 6] reveal decreasing multifractal patterns.

Fig. 3, panels (c) and (d), depict the results for the trend and bias parameters g_2 and b_2 , respectively, and report a very robust and strong pattern of the multifractal behavior for the model. The multifractality due to the correlation structure strongly increases in the 'South-East' direction from the benchmark [6, 6] positions, i.e., increasing both parameters. Already for the benchmark $g_2 = 0.4$ and $b_2 = 0.469$, the ratio of 6.7 represents a strongly significant multifractality strength as captured by the 99% confidence level that it is indeed statistically higher than 1. For higher parameterizations of b_2 , even lower

values of g_2 still reveal strong and statistically significant multifractality driven by a complex agent-based structure of the model.

Assessment of the statistical significance of multifractality differences across the grid of parametrizations can be found in Fig. B.11, panels (a) and (b). In both cases, most or parametrizations lead to strongly statistically significantly different multifractality ratios. Still, there are apparent ‘border lines’ linked to the benchmark positions [9, 6] and [6, 6] that naturally separate areas with lower and higher multifractality as detected above.

To summarize, our results reveal that a partially puzzling behavior and a ‘negative’ conclusion about the multifractal characteristics of the Brock and Hommes (1998) model in Kukacka and Kristoufek (2020) are markedly parameterization-specific. Under the increasing intensity of choice γ and/or the bias b_2 and trend g_2 parameters, we observe a significant multifractality suggesting high and even increasing complexity of the model.

5.2.2. Gaunersdorfer and Hommes (2007) model for volatility clustering

Fig. 4, panels (a) and (b), depict the results for the fundamentalists’ parameter ν and the trend-following parameter w . The benchmark [6, 11] positions reveal a considerable multifractality strength of 4.6 (panel a), which is statistically significantly higher than 1 at the 96% confidence level (panel b). Importantly, only the benchmark value $\nu = 1$ in combination with above-benchmark values of w and the value $\nu = 0.99$ exhibit statistically significant multifractal behavior based on confidence levels $\geq 95\%$. The multifractality strength and confidence level then slightly increase with increasing w while both metrics clearly deteriorate with decreasing both parameters.

Fig. 4, panels (c) and (d), depict the results for the intensity of choice γ and the trend following the correction term ψ . The multifractality behavior due to the agent-based correlation structure of the model generally increases and becomes statistically significant in the ‘South-West’ direction from the benchmark [6,6] positions, i.e., with increasing ψ surprisingly supported by decreasing γ . In other words, both a higher mispricing penalty and a less intensive switching of agents between trading strategies likely slow down the dynamic behavior of the model, which markedly supports its multifractal features.

Statistical significance of multifractality differences across the grid can be found in Fig. B.11, panels (c) and (d). The former reports a clear statistical significance for almost all parametrizations except the ones in the closest surroundings of the benchmark [6, 11] position, while the latter reveals a relatively wide, slightly downward-sloping band of statistical insignificance separating areas with lower and higher multifractality as detected above.

To summarize, our grid analysis considerably extends and enriches the parameterization-specific results of Kukacka and Kristoufek (2020). Surprisingly, the multifractal behavior of the model is mostly associated with increasing the mispricing correction term ψ and decreasing the intensity of choice γ . This is rather counterintuitive as it contradicts results for the original Brock and Hommes (1998) model in which an increasing complexity of the model is associated with increasing intensity of choice (see Section 5.2.1). Also, increasing the trend-following parameter w leads to a significant multifractality for the two highest values of the fundamentalists’ parameter ν , i.e., for models with (almost) completely naive fundamental forecasters.

5.3. ‘Ant’ herding dynamics family

5.3.1. Gilli and Winker (2003) model of herding

Fig. 5, panels (a) and (b), depict the results for the transition probabilities ε and ρ . While the benchmark [6, 6] positions suggest a considerable multifractality strength of 7.8 (panel a) but the respective confidence level of 89% (panel b) remains beyond standard statistical significance levels. However, we can observe a clear pattern of the multifractality changes in the grid of parameters. The multifractality strength generally increases in the ‘South-East’ direction and markedly decreases in the ‘South-West’ direction from the benchmark [6, 6] positions, i.e., it generally increases/decreases with increasing/decreasing spontaneous switching probability ε supported, in addition, by the increasing recruitment probability ρ . The confidence levels (panel b) suggest that the key multifractal parameter in the model is the spontaneous switching probability ε since only for its above-benchmark values does the model exhibit a statistically significant multifractality due to an agent-based correlation structure, as captured by the levels ≥ 0.95 . The confidence levels also slightly decrease with increasing the probability ρ but at a considerably slower speed.

Fig. 5, panels (c) and (d), depict the results for the adjustment speed ϕ to the fundamental price and the number of agents N in the model. In general, while the multifractality strength due to the correlation structure of the model increases with the growth of both parameters (panel c), it only gains statistical significance with the decreasing number of agents N (panel d).

Fig. B.11, panels (e) and (f) detect large subsets of the grid parametrizations leading to statistically indifferent multifractality levels. The multifractality differences gain statistical significance only in the directions of a considerable decrease or increase of the multifractality strength.

To summarize, one of the key parameters responsible for the complex behavior of the Gilli and Winker (2003) model is the probability of a spontaneous switching ε for which an increase gives rise to statistically significant multifractal behavior. For high values of ε , the probability of successful recruitment ρ further contributes to the complexity of the model. These

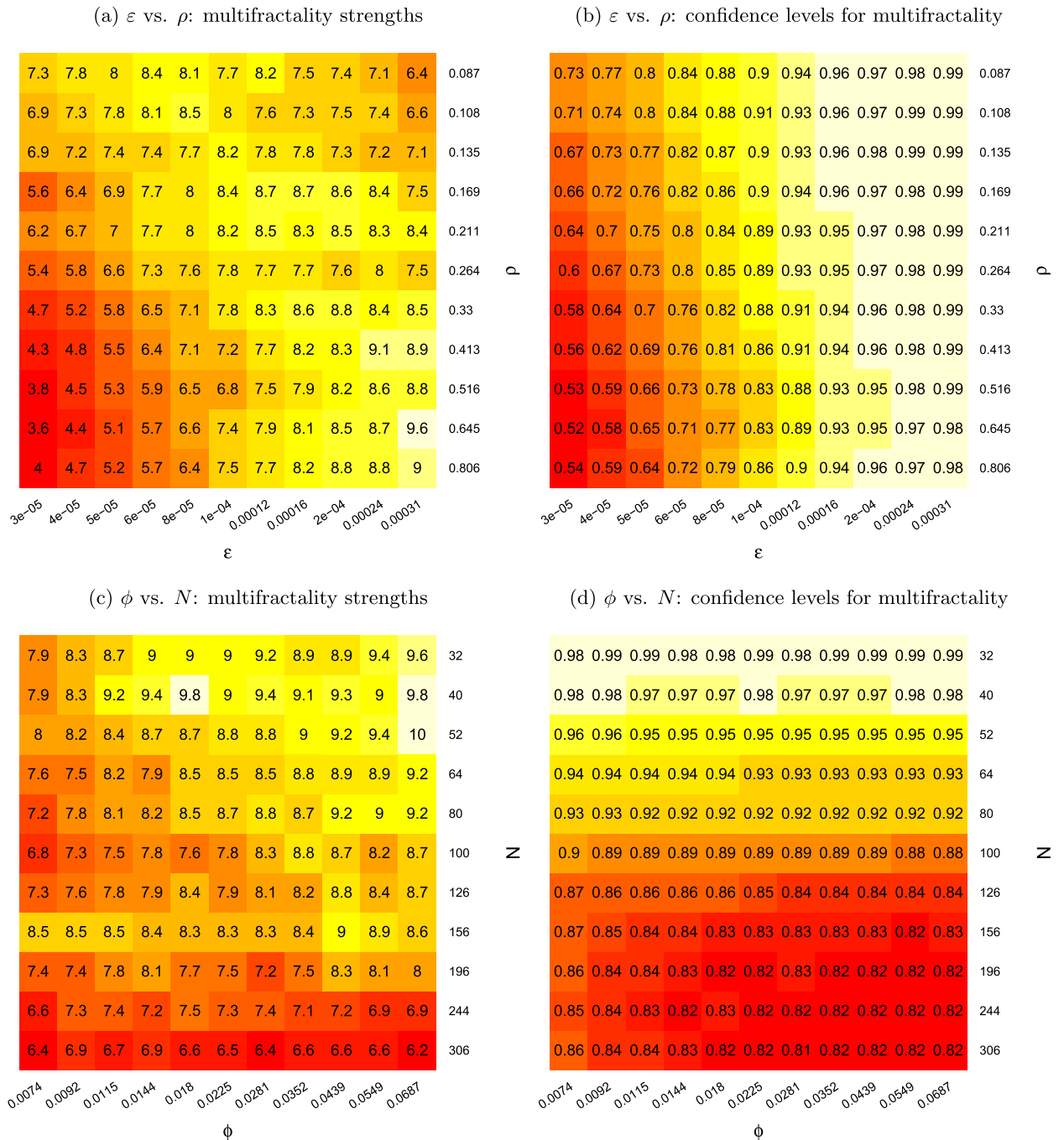


Fig. 5. Results for the *Gilli and Winker (2003)* model *Note:* The heat map color gradually changes from red (dark) to pale as the displayed value increases. The multifractality strength > 1 and the confidence level for multifractality ≥ 0.95 indicate the presence of a statistically significant multifractality due to a complex agent-based correlation structure at the 5% level. The presented values are based on 1000 random runs and rounded to one and two decimal digits. The confidence level 0.99 stands for ≥ 0.99 . Depicted parameters: ε ...spontaneous switching probability; ρ ...recruitment probability; ϕ ...fundamentalists' adjustment speed; N ...number of agents. (For interpretation of the references to colour in this figure legend, the reader is referred to the web version of this article.)

results confirm our expectation about a positive impact of the switching probabilities on the model complexity. Contrary to our expectation, the number of agents N appears negatively associated with the model's complexity as only low values of N lead to strongly significant multifractality.

Regarding ε_1 and ε_2 , the multifractality due to the model correlation structure markedly increases from the benchmark [6, 6] position as ε_1 decreases while ε_2 remains stable or increases. Thus, the two parameters governing spontaneous switching probability seem to have an opposite impact on the model complexity, at least in a subsector of the grid lattice of model parameterizations.

Fig. 6, panels (c) and (d), depict the results for ε_1 governing the spontaneous switching probability for fundamentalists, and the recruitment probability/herding tendency ρ . For the above-benchmark combinations of both parameters, the model numerically diverges; however, we can observe a clear pattern of the multifractality changes in the remaining two quadrants of the parameters grid. The model complexity clearly increases and gains statistical significance in the ‘North-West’ direction from the benchmark [6,6] position, i.e., with ε_1 decreasing while ρ increases.

Assessment of the statistical significance of multifractality differences across the grid of parametrizations can be found in Fig. B.11, panels (g) and (h). In both cases, most or parametrizations lead to strongly statistically significantly different multifractality ratios but there are apparent insignificant ‘border lines’ linked to the benchmark positions that separate areas with lower and higher multifractality detected above.

To conclude, our analysis again markedly extends the parameterization-specific results of Kukacka and Kristoufek (2020) where the Alfarano et al. (2005) model displays a puzzling multifractal behavior. The two crucial parameters triggering multifractal behavior of the model are the ε_1 decreasing the fundamentalists’ spontaneous switching probability and the increasing herding tendency ρ . The latter results follow our expectations as well as agree with the results for the Gilli and Winker (2003) model from the same ant mechanics family. The former also makes intuitive sense, although it is consistent with the results of the previous model only in the decreasing direction.

5.3.3. Alfarano, Lux, and Wagner (2008) model

Fig. 7, panels (a) and (b), depict the results for the a intensity of autonomous switches and b herding rate. The benchmark [6, 6] positions suggest a considerable multifractality strength of 3.5 (panel a), but the respective confidence level of 86% (panel b) remains beyond standard statistical significance levels. However, one can observe a clear pattern of an increasing multifractality due to the agent-based correlation structure in the ‘South-East’ direction, i.e., with increasing both key parameters while decreasing in the opposite direction. For combinations with higher values of calibrated parameters, it also clearly gains statistical significance.

Fig. 7, panels (c) and (d), depict the results for the standard deviation σ_f and the number of noise traders n_c . Surprisingly, in contrast to our expectations, the number of noise traders does not impact the complexity of the model. The numerical differences in the individual columns of panels (c) and (d), to which different parameterizations of n_c are associated, can be safely attributed to the stochastic nature of the Monte Carlo analysis. The impact of the standard deviation σ_f then seems to follow our latter explanation, i.e., the decreasing magnitude of innovations leads to higher predictability. We observe a statistically significant multifractal behavior for the four lowest parameter values of $\sigma_f = \{0.01, 0.012, 0.015, 0.019\}$.

Similarly to the Alfarano et al. (2005) model, Fig. B.11, panels (i) and (j) detect clear ‘border lines’ across the grid that separate areas with statistically significantly lower and higher multifractality detected above.

To conclude, this sensitivity analysis markedly enriches the knowledge about the complex behavior of the Alfarano et al. (2008). The two crucial parameters governing the dynamics of the model, the intensity of autonomous switches a and the herding rate b , can also trigger statistically significant multifractal behavior under the parameter combination with high values. Surprisingly, the number of noise traders who switch between the optimistic and pessimistic mood, i.e., the model’s dynamic core, does not impact the model complexity. Finally, the magnitude of the fundamental innovations σ_f can increase the system’s complexity via its stabilization.

5.4. Structural stochastic volatility family

5.4.1. Franke and Westerhoff (2011) structural stochastic volatility model

Fig. 8, panels (a) and (b), depict the results for the price misalignment parameter a_d and the flexibility parameter ν . The benchmark [6, 6] positions suggest a considerable multifractality strength of 5.6 (panel a), and panel (b) provides evidence of its ≥ 0.99 statistical confidence. The model thus exhibits strongly statistically significant multifractal features directly under the benchmark parameterization. We can then observe further slight evolution of increasing multifractality in the ‘North-West-West’ direction from the benchmark [6, 6] positions, i.e., with decreasing both the price misalignment parameter and the flexibility parameter. On the other hand, especially in the ‘North-East’ direction, i.e., with increasing the price misalignment parameter while decreasing the flexibility parameter, the model generally loses its multifractal properties.

Fig. 8, panels (c) and (d), depict the results for the adjustment parameters for fundamentalists (ϕ) and chartists (χ), respectively. In contrast to our expectations, χ does not seem to have any important impact on the model complexity as directly seen from the ‘column-shaped’ structure of Fig. 8. On the other hand, the multifractality tends to slowly grow from the benchmark [6, 6] positions with increasing ϕ . On the contrary, it gradually declines with decreasing ϕ and even deteriorates w.r.t. the statistical confidence for its smallest values.

Assessment of the statistical significance of multifractality differences across the grid of parametrizations can be found in Fig. B.11, panels (k) and (l). Importantly, the slight evolution of increasing multifractality in the ‘North-West-West’ direction detected in Fig. 8, panels (a), see above, is only associated with an unclear significance pattern at the 5% level. On the other hand, the multifractality decrease in the ‘North-East’ direction is clearly statistically significant. Panel (l) then displays a

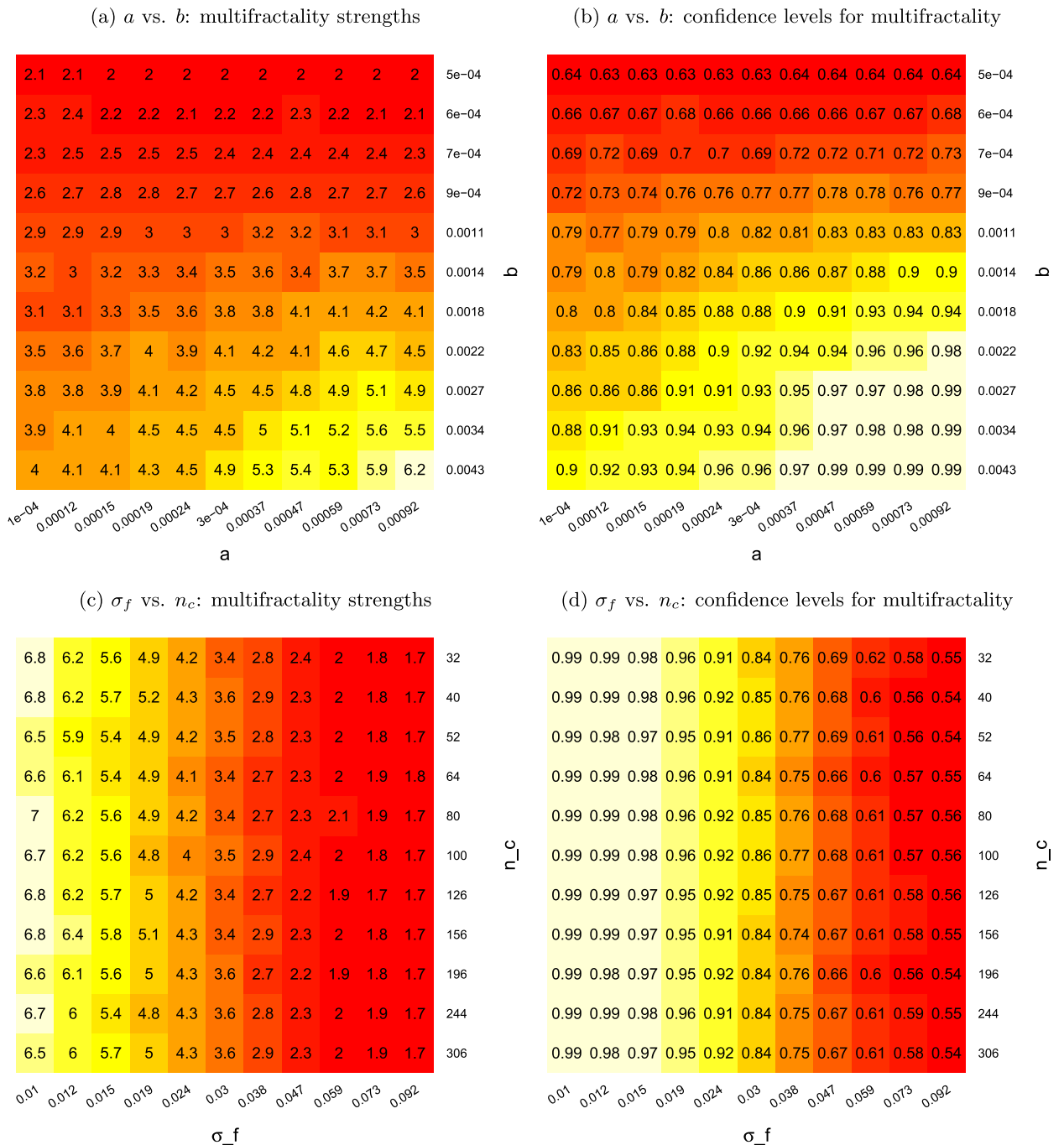


Fig. 7. Results for the Alfarano et al. (2008) model Note: The heat map color gradually changes from red (dark) to pale as the displayed value increases. The multifractality strength > 1 and the confidence level for multifractality ≥ 0.95 indicate the presence of a statistically significant multifractality due to a complex agent-based correlation structure at the 5% level. The presented values are based on 1000 random runs and rounded to one and two decimal digits. The confidence level 0.99 stands for ≥ 0.99 . Depicted parameters: a ...intensity of autonomous switching; b ...herding rate; σ_f ...standard deviation of fundamental innovations; n_c ...number of noise traders. (For interpretation of the references to colour in this figure legend, the reader is referred to the web version of this article.)

similar pattern observed for the Alfarano et al. (2008) model with, in this case, a relatively wide, vertical band separating areas with statistically higher and lower multifractality.

To summarize, our analysis confirms statistically significant multifractal features of Franke and Westerhoff (2011) for a robust grid of parameter values. The crucial drivers of the model complexity are, in line with our expectations, the decreasing price misalignment parameter a_d and increasing adjustment parameters for fundamentalists ϕ , both stabilizing the model

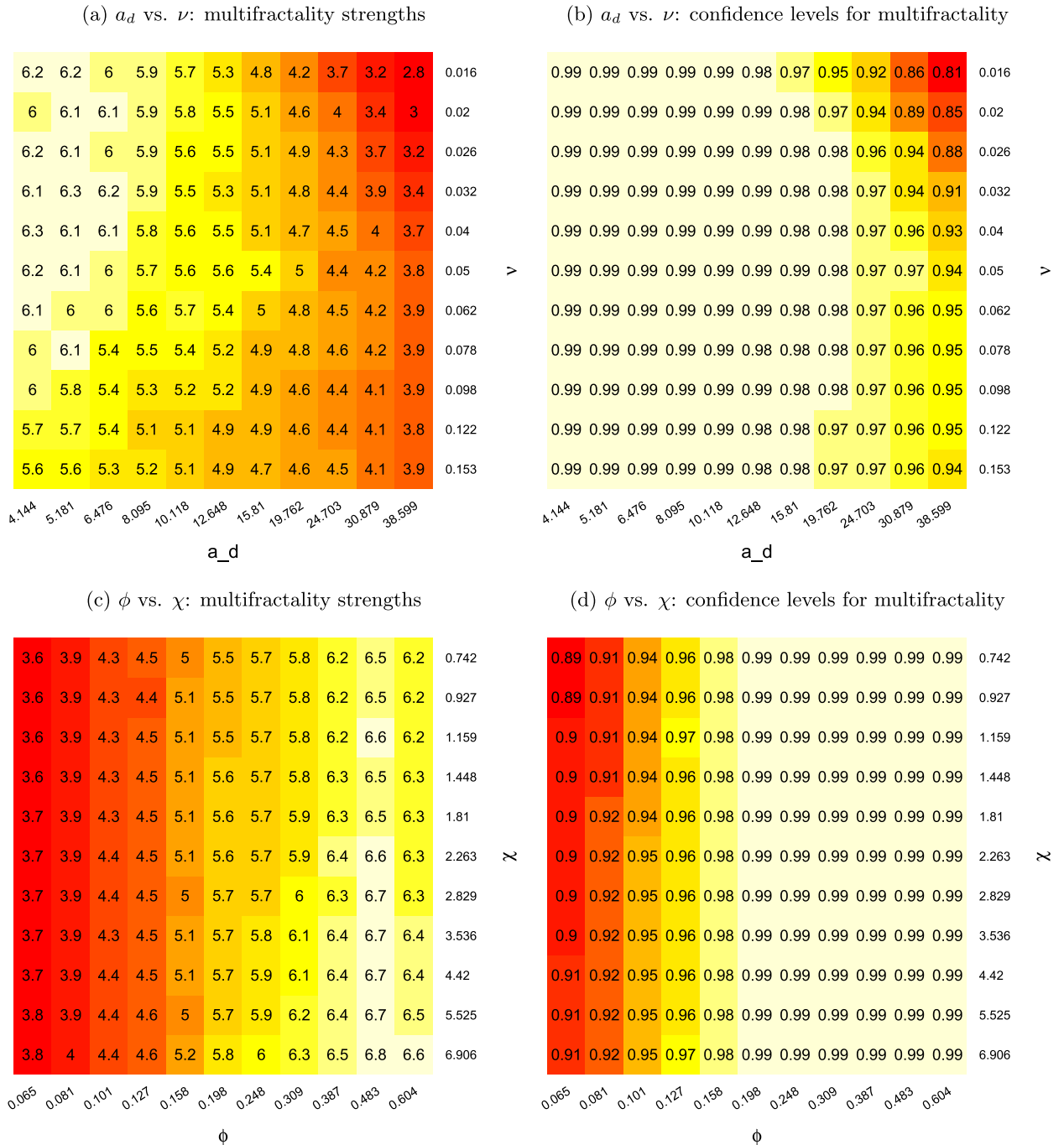


Fig. 8. Results for the Franke and Westerhoff (2011) model Note: The heat map color gradually changes from red (dark) to pale as the displayed value increases. The multifractality strength > 1 and the confidence level for multifractality ≥ 0.95 indicate the presence of a statistically significant multifractality due to a complex agent-based correlation structure at the 5% level. The presented values are based on 1000 random runs and rounded to one and two decimal digits. The confidence level 0.99 stands for ≥ 0.99 . Depicted parameters: a_d ...price misalignment parameter; ν ...flexibility parameter; ϕ ...fundamentalists' adjustment parameter; χ ...chartists' adjustment parameter. (For interpretation of the references to colour in this figure legend, the reader is referred to the web version of this article.)

dynamics. Surprisingly, parameters ν and χ with a destabilizing impact that support the model dynamics do not seem to have any important impact on model complexity.

5.4.2. Schmitt and Westerhoff (2017) model with sunspots

Fig. 9, panels (a) and (b), depict the results for the probabilities S^C, S^F . The benchmark [6, 6] positions reveal a considerable multifractality strength of 3.5 (panel a), which is statistically significantly higher than 1 at the 97% confidence level

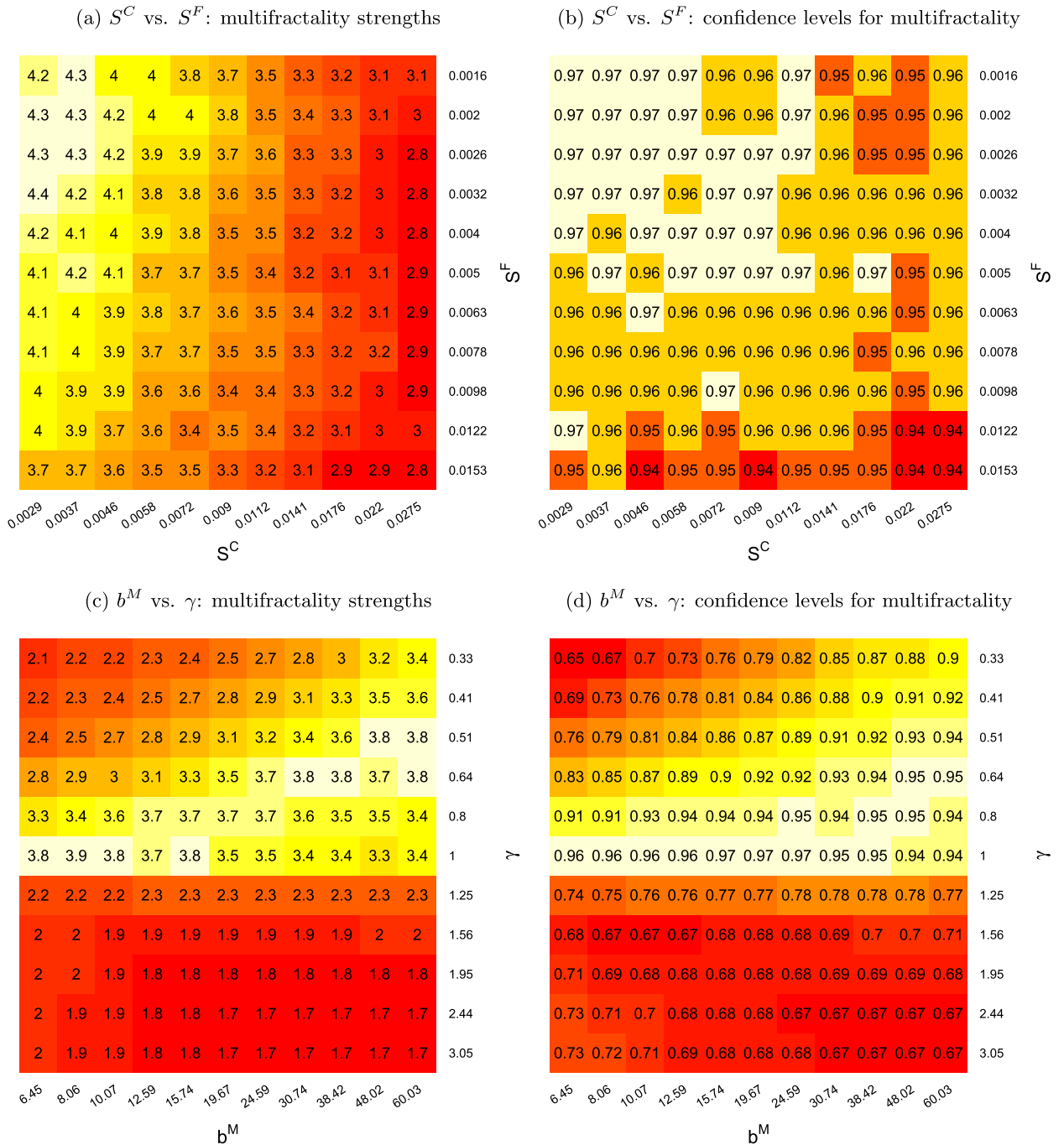


Fig. 9. Results for the Schmitt and Westerhoff (2017) model Note: The heat map color gradually changes from red (dark) to pale as the displayed value increases. The multifractality strength > 1 and the confidence level for multifractality ≥ 0.95 indicate the presence of a statistically significant multifractality due to a complex agent-based correlation structure at the 5% level. The presented values are based on 1000 random runs and rounded to one and two decimal digits. The confidence level 0.99 stands for ≥ 0.99 . Depicted parameters: S^C ...chartists' sunspot probability; S^F ...fundamentalists' sunspot probability; b^M ...price misalignment parameter; γ ...intensity of choice. (For interpretation of the references to colour in this figure legend, the reader is referred to the web version of this article.)

(panel b). We can then observe a regular but slight tendency to multifractality increase in the 'North-West' direction, i.e., with decreasing both sunspot events probabilities, which follows our expectation. Moreover, according to panel (b), statistical significance at the 5% level is reached under most of the parameterizations.

Fig. 9, panels (c) and (d), depict the results for the price misalignment parameters b^M and the intensity of choice γ . The results suggest that the benchmark [6.6] parameterization and its close neighborhood, especially $\gamma = 1$, gives rise to almost the highest and statistically significant multifractality at the 5% level. Importantly, the multifractality strength and

the related confidence level generally strongly deteriorate for above-benchmark values of γ as well as in the ‘North-West’ direction, i.e., for the smallest values of γ when combined with the smallest values of b^M .

Similarly to the Gaunersdorfer and Hommes (2007) model, panel (d), Fig. B.11, panels (m) and (n) detect wide ‘border lines’ across the grid that naturally contain the benchmark [6, 6] positions and separate areas with statistically significantly lower and higher multifractality detected above.

To conclude, our analysis enriches the parameterization-specific knowledge about the multifractal properties of the Schmitt and Westerhoff (2017) model obtained by Kukacka and Kristoufek (2020). There is a slight impact of the sunspot probabilities S^C , S^F ; however, a statistically significant multifractal behavior is only observed for the benchmark parameterization and its close neighborhood, especially for $\gamma = 1$.

6. Discussion and conclusions

6.1. Generalization of results

The multifractal sensitivity analysis of the heterogeneous set of nine financial agent-based models delivers several common results or general patterns regarding the influence of the parameter values on model complexity. For most of the models, our findings markedly extend the parameterization-specific results of Kukacka and Kristoufek (2020). However, for the cusp catastrophe model (Fig. 1), the Bornholdt (2001) Ising model (Fig. 2), and to some extent for the Schmitt and Westerhoff (2017, Figure 9) model with sunspots, only a nondescript impact of model parameterization on their complexity can be observed. Surprisingly, such a conclusion regards the oldest models (cusp catastrophe, Ising, see Section 4.1) as well as the most recent model of our set. One might suggest that the complexity of financial agent-based models likely increases over time as more complicated modeling frameworks are being developed. Our analysis, however, argues that this is not a general tendency since already some of the first financial agent-based models have exhibited very complex behavior under specific parameterizations, and the pattern of an overall multifractality strength goes up and down in time.

Our updated methodology for multifractality detection further helps to uncover a richer multifractal behavior for the Gaunersdorfer and Hommes (2007), Alfarano et al. (2005), and Schmitt and Westerhoff (2017) models even under their benchmark parameterizations (see Figs. 4, 6, 9) which appeared puzzling or statistically insignificant at the 5% level in Kukacka and Kristoufek (2020). Although, this paper does not study the increasing ability of multifractality detection with increasing sample size, which we keep fixed in our sensitivity analysis. For the other five not yet mentioned models, we observe patterns of complexity evolution associated with specific model parameters. This is an especially important result for the Brock and Hommes (1998, Figure 3) model that, under the benchmark parameterization, does not meet the multifractal criteria of the Kukacka and Kristoufek (2020) analysis and displays a partially puzzling behavior.

6.2. Common findings and apparent contradictions

As the four suggested model families (see Table 2) share similar modeling concepts, it is crucial to study some generally observed patterns or, on the other hand, apparent contradictions. For this purpose, one always needs to consider the intersection of information contained in all three heat maps for each parameter combination. First, we can conclude that parameters associated with the herding behavior of agents represented by the recruitment probability (Gilli and Winker, 2003, Figure 5 (a) and (b), par. ρ) or herding rate (Alfarano et al., 2008, Figure 7 (a) and (b), par. b) generally exhibit a strong impact on model complexity as their increase leads to increase and statistical significance of multifractality. For the Alfarano et al. (2005, Figure 6 (c) and (d), par. ρ) model, increases of the recruitment probability lead to numerical divergence, but its decrease is also associated with statistically significant changes of the multifractality strength. This is an intuitive result since the herding behavior is likely associated with the formation of complex agent-based correlation structures. A similar impact can be clearly observed for the Adaptive belief system family for increasing trend extrapolation parameters (Fig. 3 (c) and (d), par. g_2 ; and Fig. 4 (a) and (b), par. w), essentially replacing the herding mechanism within the multinomial logistic switching framework.

Second, various parameters with a stabilizing impact, e.g., memory in the Brock and Hommes (1998, Figure 3 (a) and (b), par. ρ) model, the mispricing correction parameter in the Gaunersdorfer and Hommes (2007, Figure 4 (c) and (d), par. ψ) model, the decreasing intensity of fundamental innovations in the Alfarano et al. (2008, Figure 7 (c) and (d), par. σ_f) model, decreasing price misalignment and flexibility parameters in the Franke and Westerhoff (2011, Figure 8 (a) and (b), par. a_d and ν) model, or decreasing sunspot probabilities in Schmitt and Westerhoff (2017, Figure 9 (a) and (b), par. S^C and S^F) strongly support the complexity of the given models and its statistical significance therein. In a similar vein, parameters generally positively associated with the population of fundamental traders, i.e., again related to the stabilizing tendencies, also support multifractal properties of most models where applicable (Gaunersdorfer and Hommes, 2007; Gilli and Winker, 2003; Franke and Westerhoff, 2011, see Figures 4, 5, 8, par. ν , ϕ) but not always (Alfarano et al., 2005, Figure 6, par. ε_1). Both of the latter results seem intuitive because various stabilization tendencies make the system less stochastic, leading to higher predictability.

On the other hand, for ‘other or opposite then highlighted’ areas of the parameterization grid, the analyzed models generally do not generate statistically significant multifractal dynamics. Moreover, the intensity of choice, one of the core drivers

of the dynamics of many financial agent-based models, seems to have a potentially strong but strictly model-specific impact: it is strongly positively related to model complexity in the Brock and Hommes (1998, Figure 3 (a) and (b), par. γ) model, but it does not exhibit any considerable impact in the Gounersdorfer and Hommes (2007) and Schmitt and Westerhoff (2017) models (see Figs. 4, 9, par. γ). Next, an increasing number of agents does not have any statistically significant impact on the model complexity in the Alfarano et al. (2008, Figure 7 (c) and (d), par. n_c) model. An opposite tendency is, however, observable for Gilli and Winker (2003, Figure 5 (c) and (d), par. N). This is a surprising result since one might expect that more interacting agents will likely give rise to multifractal correlation structures in general. Finally, the parameters associated with the population of chartists, i.e., related to generally destabilizing tendencies in the markets, seem to harm the model complexity in the cusp catastrophe model (Fig. 1, par. β_2), a positive impact in the Brock and Hommes (1998, Figure 3 (c) and (d), par. g_2 and b_2) model, and no important effect on the model complexity in the model by Alfarano et al. (2005, Figure 6 (a) and (b), par. ε_2).

6.3. Agent-based mechanisms leading to multifractality

While none of the oldest models inspired by other scientific disciplines generates statistically significant multifractal behavior, all other models from the remaining three families are associated with statistically significant multifractality in a specific subset of their parametrization grid. Therefore, a distinguishing feature ultimately driving the model complexity seems to be the implementation of a switching mechanism governing agents' interactions. For the Adaptive belief system family and the model by Schmitt and Westerhoff (2017), this is represented by the multinomial logistic formula (15,17, and 26) whose impact is governed by the intensity of choice. For the 'Ant' herding dynamics family (Section 4.3), it can be proxied by the autonomous switching and recruitment probabilities, or the herding rate. As the probability of autonomous switching is essentially an opposite concept to the herding behavior, it most likely affects the model complexity through a different transmission channel than herding, e.g., by supporting nonlinear dynamics of given models. Finally, in the Structural stochastic volatility family (Section 4.4), the switching mechanism is represented by the switching index.

When aggregated information from all three types of heat maps is considered, the Gounersdorfer and Hommes (2007, Figures 4 and B.11) and Alfarano et al. (2008, Figures 7 and B.11) models are perhaps the two most robustly associated with a complex, statistically significant multifractal behavior and with a significant impact of the parameterization changes on the model complexity. For these two models, we summarize the 'sufficient' parametric conditions for the presence of multifractality. According to Fig. 4 for the Gounersdorfer and Hommes (2007) model, considering the fundamentalists' parameter ν and chartists' trend-following parameter w , we observe the emergence of a statistically significant multifractality at the 5% level for any w under $\nu = 0.99$ and for larger $w \geq 1.9$ under $\nu = 1$ which is the borderline value of the grid. Actually, the second pair of values represent the benchmark parameterization at the [6, 11] position. For the nexus between the intensity of choice γ and the trend followers' mispricing correction term ψ , any value of γ combined with $\psi \geq 1800$, which again resembles the benchmark parameterization, leads to a statistically significant multifractality. Both findings support the necessity and sufficiency of strong stabilizing factors for the multifractality emergence for this model. According to Fig. 7 for the Alfarano et al. (2008) models, considering the intensity of autonomous switching a and the herding rate b , we observe the emergence of multifractality roughly for the above-benchmark levels of both parameters, i.e., for combinations of a strong herding tendency with strong autonomous switching. For the nexus between the intensity of standard deviation of fundamental innovations σ_f and the number of noise traders n_c , any value of n_c combined with $\sigma_f \leq 0.019$ leads to a statistically significant multifractality. These results further support the importance and sufficiency of a strong stabilizing tendency represented by low σ_f together with intensive switching and herding behavior of agents.

6.4. Seemingly puzzling multifractality strength below one

For the Bornholdt (2001) Ising model, the responsiveness parameter setup $\beta = 0.22$ is associated with a seemingly puzzling multifractality strengths (see Fig. 2 (a)) clearly below 1. This is a numerical result without any theoretical rationale since the level of multifractality in the randomly shuffled series considered in the denominator of the individual multifractality strength ratios should generally be lower or the same as that of the original simulated series.

However, an occasionally lower level of multifractality estimated for the original simulated series can be explained because some models are more likely to generate negatively autocorrelated returns for some parameter combinations. This is caused by a strong mean-reverting model dynamics or even 'wild jumping' up and down under various unrealistic parameterizations. This seemingly puzzling phenomenon is studied, e.g., in Barunik et al. (2012) for the generalized Hurst exponent estimation method, and we presuppose a similar behavior also for the MF-DFA.

Table A.3 confirms this suspicion as the 90% sample confidence interval of the estimated AR(1) coefficient for the Ising model is completely negative. As Table A.3 only contains statistics for the benchmark parametrization, we also estimate the Ising's AR(1) coefficient for one of the apparently affected parametrizations: $\beta = 0.22$, $\alpha = 4$, which also gives completely negative 90% sample confidence interval $(-0.15; -0.13)$.

For several other models, namely by Gilli and Winker (2003), Alfarano et al. (2005, 2008), and Schmitt and Westerhoff (2017), the confidence interval of the estimated AR(1) coefficient also interferes with negative values. Therefore, a similar phenomenon might partially affect the multifractality strength results for other models, especially under parametrizations associated with low confidence levels. Still, the impact on the Bornholdt (2001) Ising model is by far the most apparent

one because, for other potentially affected models, it never translates to the numerical value of the multifractality strength below 1.

6.5. Realism of parameterizations and future outlook

A straightforward avenue for potential future research is assessing how realistic the parameterizations for individual models leading to agent-based-driven multifractal behaviors actually are. This is important, especially for the parameterizations relatively far away from the benchmark settings suggested in the original research papers or the follow-up research articles studying their behavior. However, it needs to be noted that such research, provided that the identical methodology is used, would need to focus on a smaller subset of models to make the endeavor realistic and computationally bearable.

As our results show that various complex dynamics are observed not only for the benchmark parameter settings but also for many other combinations of parameter values, one of the natural future steps under the computational limits of the current methodology might focus on a specific model or a family of models. Through the study of its ability to replicate other financial stylized facts concerning the parameter setting, one should obtain a more comprehensive picture and ascertain whether the ‘success’ in one area does not lead to impractical and unrealistic properties in other important dynamic and/or distributional properties of the model-generated series. One such example, albeit still rather limited, is [Kristoufek and Vosvrda \(2018\)](#) who study the Efficient Market Hypothesis, i.e., no autocorrelation and Gaussian distribution of returns, of the [Bornholdt \(2001\)](#) Ising model and show that other parameter combinations are leading to a setting that is realistic from the financial perspective but not previously discussed. Building on such detailed studies of specific models, we could eventually arrive at important policy or structural implications for financial markets and, in turn, make financial agent-based models more appealing and influential.

Another promising future research direction that could overcome the computational limitations of the current grid search experimental design is taking advantage of a surrogate modeling method ([Lamperti et al., 2018](#)). This approach based on Sobol sampling would lead to a considerably more efficient search over the parameter space, allowing for relatively quick identification of interesting regions, for a more detailed analysis combining multiple parameters in more dimensions, or for a more ‘granular’ focus. However, such a conceptual methodological advancement would bring new layers of necessary ‘training’ of each surrogate model and additional analysis of the sufficient surrogate model approximation. It also needs to be verified what potential impact on the multifractal features of individual models such a surrogate modeling approach might bring and whether it does not alter properties of multifractality estimators. Therefore, a proper analysis of the given approach must be completed before its implementation within the multifractality estimation.

Code availability

Supplementary material associated with this article containing R code for the MF-DFA estimator of the generalized Hurst exponent, R code for an illustrative replication of the results for the [Gauersdorfer and Hommes \(2007\)](#) model ([Section 4.2.2](#), [Section 5.2.2](#)) together with the respective output, and the scripts to produce the presented heat map graphics can be found on GitHub at the following address: github.com/jirikukacka/Kukacka_Kristoufek_2021 [created 2021-05-25].

Declaration of Competing Interest

None.

Acknowledgment

We gratefully acknowledge financial support from the Czech Science Foundation under the ‘Multifractality analysis in finance’ project [17-12386Y] and from the Charles University PRIMUS program [project PRIMUS/19/HUM/17]. Kukacka gratefully acknowledges financial support from the Charles University UNCE program [project UNCE/HUM/035]. The MATLAB code of the ALW (2008) model has been kindly provided by Prof. Thomas Lux (University of Kiel, Germany) and Dr. Zhenxi Chen (South China University of Technology). The MATLAB codes of the GW (2003), ALW (2005), and FW (2011) models have been kindly provided by Dr. Sylvain Barde (University of Kent, UK). The *Mathematica* code of the SW (2017) model has been kindly provided by Prof. Frank Westerhoff (University of Bamberg, Germany). The MATLAB code of the GH (2007) model has been downloaded from the [agentFin 0.1 documentation](#) web page [accessed 2019-10-28] by Prof. Blake LeBaron (Brandeis University, USA). This paper has benefited from discussions with participants at the 24th Annual Workshops on Economic Science with Heterogeneous Interacting Agents in London (2019) and the 24.5th Workshop on Economics with Heterogeneous Interacting Agents (2021, online). Finally, we are very thankful to the two anonymous reviewers for their inspiring comments and detailed suggestions.

Appendix A. Descriptive statistics and model outputs

Table A.3
Descriptive statistics.

| | Cusp (1974) | BH (1998) | Ising (2001) | GW (2003) | ALW (2005) | GH (2007) | ALW (2008) | FW (2011) | SW (2017) |
|-------------------|----------------------------|------------------------|----------------------------|------------------------|-------------------------|------------------------|------------------------|------------------------|------------------------|
| <i>Mean</i> | -0.03 (- 0.12;0.08) | 0.01 (- 0.10;0.10) | 0.00 (0.00;0.00) | 0.00 (0.00;0.00) | 0.00 (0.00;0.00) | 0.00 (0.00;0.00) | 0.00 (0.00;0.00) | 0.00 (0.00;0.00) | 0.00 (0.00;0.00) |
| <i>SD</i> | 1.18 (1.17;1.19) | 0.11 (0.11;0.11) | 0.01 (0.01;0.01) | 0.04 (0.00;0.07) | 0.01 (0.01;0.01) | 0.01 (0.01;0.01) | 0.04 (0.04;0.04) | 0.01 (0.01;0.01) | 0.01 (0.01;0.01) |
| <i>Skew</i> | 0.39 (0.37;0.41) | 0.01 (- 0.10;0.11) | 0.00 (- 0.04;0.03) | 0.48 (- 0.01;1.31) | 0.31 (- 1.57;1.34) | 0.12 (- 0.02;0.12) | 0.00 (- 0.05;0.05) | 0.00 (- 0.06;0.07) | 0.01 (- 0.51;0.54) |
| <i>Ex Kurt</i> | -0.93 (- 0.96; - 0.90) | 0.06 (- 0.01;0.13) | 0.21 (0.01;1.18) | 17.27 (0.0;73.52) | 138.74 (5.19;153.43) | 23.69 (0.91;3.61) | 0.93 (0.76;1.08) | 1.44 (1.26;1.64) | 12.51 (6.35;22.61) |
| <i>J - B</i> | 0.00 (0.00;0.00) | 0.00 (0.0;0.01) | 0.16 (0.00;0.68) | 0.03 (0.00;0.20) | 0.00 (0.00;0.00) | 0.00 (0.00;0.00) | 0.00 (0.00;0.00) | 0.00 (0.00;0.00) | 0.00 (0.00;0.00) |
| <i>ADF</i> | ≤0.01 (0.01;0.01) | ≤0.01 (0.01;0.01) | ≤0.01 (0.01;0.01) | ≤0.01 (0.01;0.01) | ≤0.01 (0.01;0.01) | ≤0.01 (0.01;0.01) | ≤0.01 (0.01;0.01) | ≤0.01 (0.01;0.01) | ≤0.01 (0.01;0.01) |
| <i>KPSS</i> | 0.01 (0.01;0.02) | 0.08 (0.01;0.10) | ≥0.10 (0.10;0.10) | 0.05 (0.01;0.10) | ≥0.10 (0.06;0.10) | ≥0.10 (0.10;0.10) | ≥0.10 (0.10;0.10) | ≥0.10 (0.10;0.10) | ≥0.10 (0.10;0.10) |
| <i>L - B</i> | 0.19 (0.00;0.78) | 0.00 (0.0;0.00) | 0.00 (0.00;0.00) | 0.00 (0.00;0.00) | 0.23 (0.00;0.85) | 0.00 (0.00;0.00) | 0.45 (0.02;0.93) | 0.21 (0.00;0.82) | 0.32 (0.00;0.91) |
| $\widehat{AR}(1)$ | 0.01 (0.00;0.03) | 0.37 (0.36;0.39) | -0.28 (- 0.30; - 0.23) | 0.31 (- 0.34;0.46) | 0.00 (- 0.03;0.03) | 0.10 (0.06;0.15) | 0.00 (- 0.01;0.01) | 0.01 (0.00;0.03) | 0.01 (- 0.01;0.02) |

Note: The results are based on 1000 random runs of the examined models under the benchmark parameterization and the general simulation setup. Resulting 90% sample confidence intervals are reported in () parentheses. p -values are reported for the statistical tests: H_0 for the Jarque-Bera test is 'normality,' H_0 for the augmented Dickey-Fuller test is 'unit root/nonstationarity,' H_0 for the Kwiatkowski-Phillips-Schmidt-Shin is 'stationarity,' and H_0 for the Ljung-Box test is 'no autocorrelation on the first lag.' $\widehat{AR}(1)$ reports the estimated AR(1) coefficient based on the ARIMA (1,0,0) model. The figures are rounded to 2 decimal places. Models are ordered chronologically.

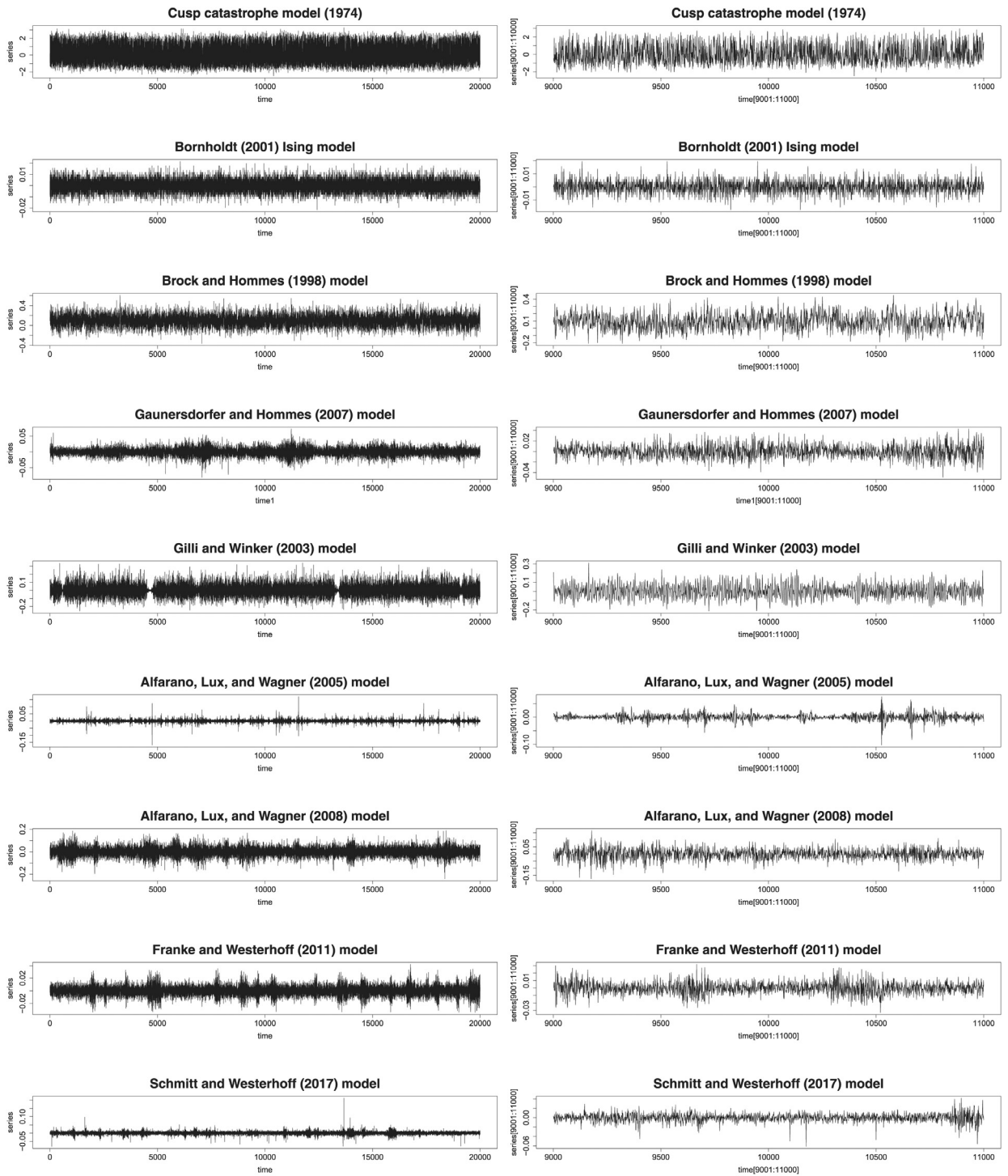


Fig. A.10. Model outputs Note: The left half of the figure displays typical time series outputs of the examined models under the benchmark parameterization and the general simulation setup. The right half zooms the respective left-hand side series for the 2000 middle observation.

Appendix B. Confidence levels for differences

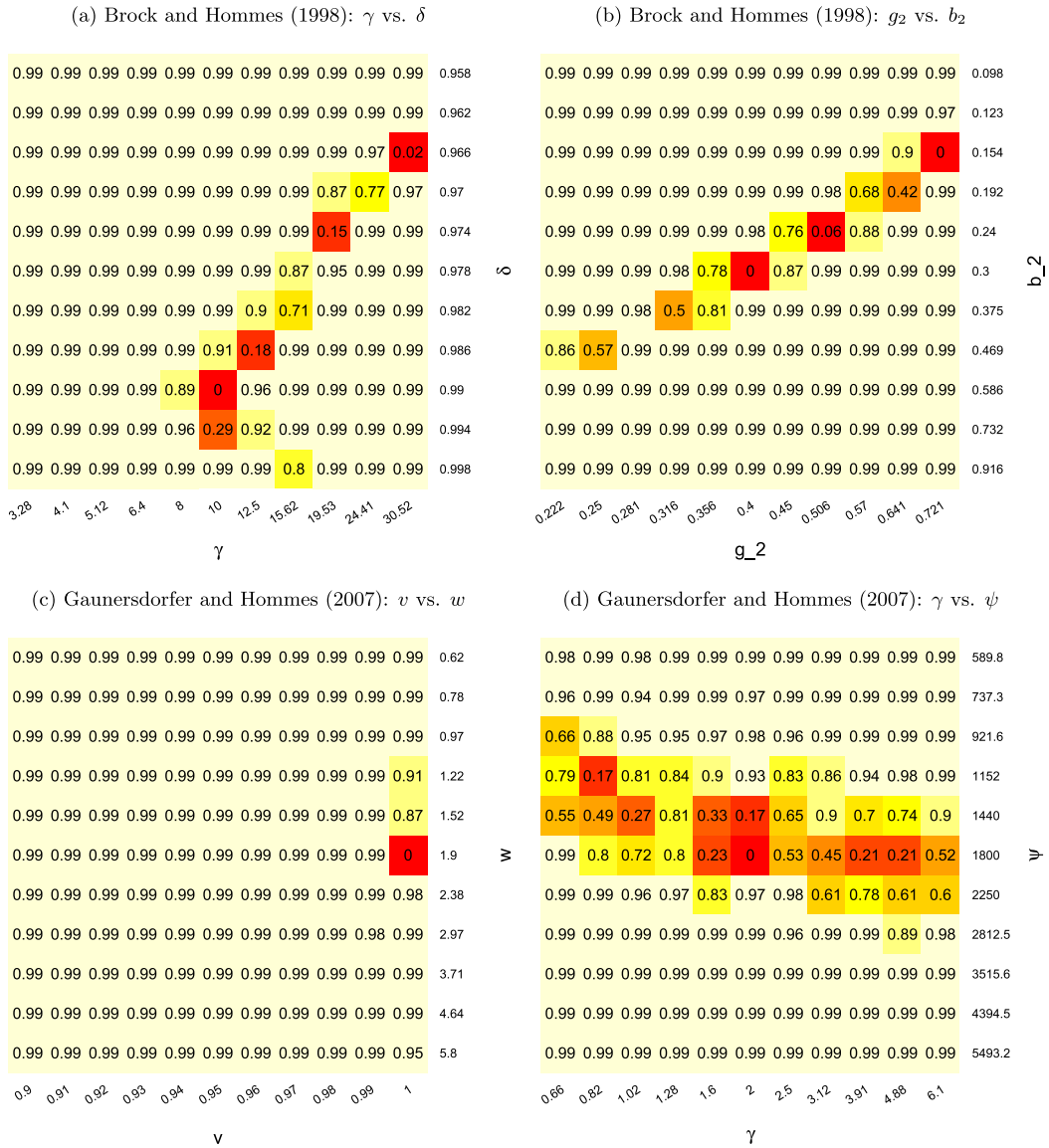


Fig. B.11. Results for the confidence levels for differences Note: The heat map color gradually changes from red (dark) to pale as the displayed value increases. The confidence level ≥ 0.95 indicate a statistically significant difference of the given multifractality ratios in Fig. 3–Fig. 9 compared to the benchmark parametrization. The presented values are based on 1000 random runs and rounded to one and two decimal digits. The confidence level 0.99 stands for ≥ 0.99 . (For interpretation of the references to colour in this figure legend, the reader is referred to the web version of this article.)

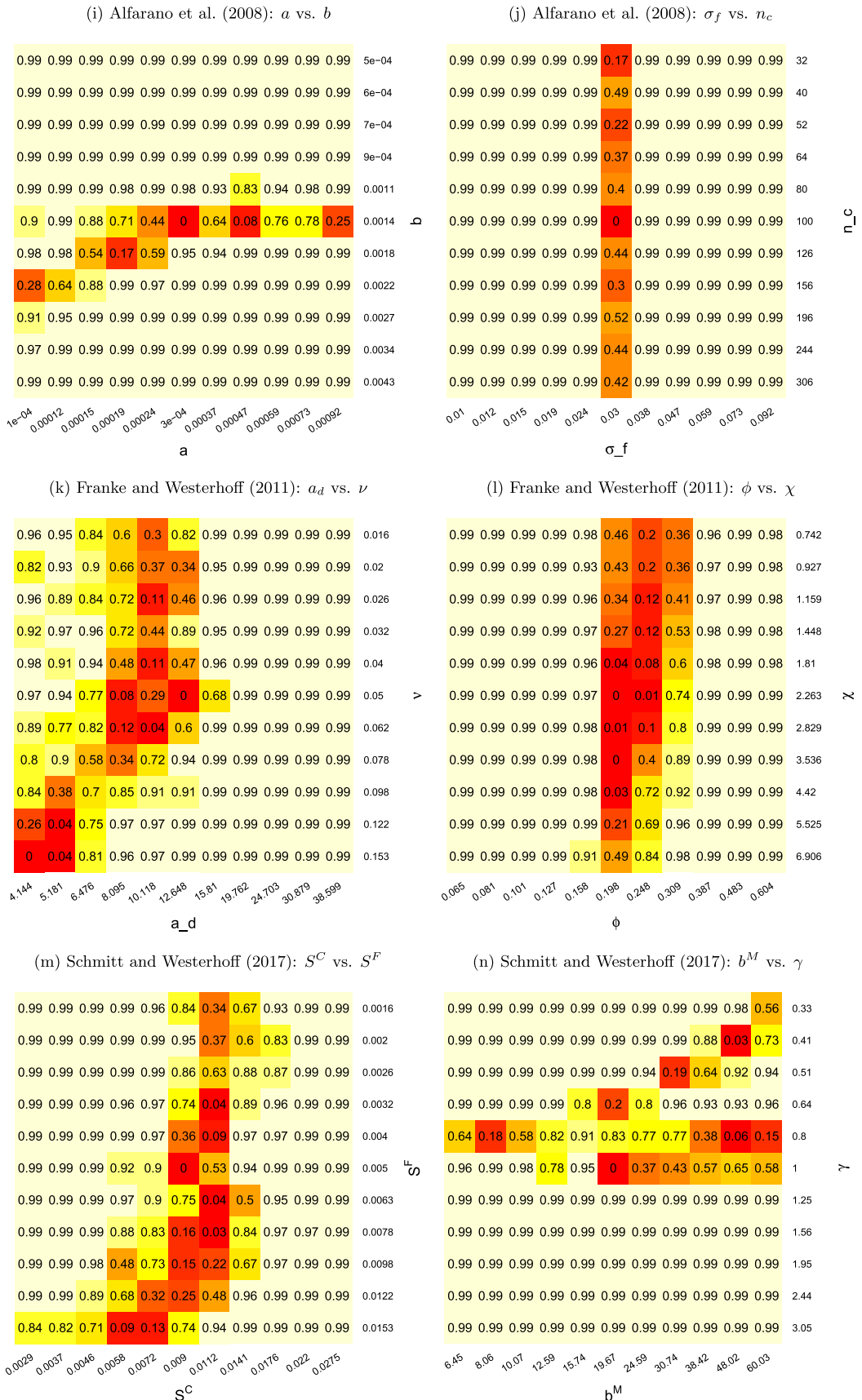


Fig. B.1135 continued

References

- Alfarano, S., Lux, T., Wagner, F., 2005. Estimation of agent-based models: the case of an asymmetric herding models. *Comput. Econ.* 26, 19–49.
- Alfarano, S., Lux, T., Wagner, F., 2008. Time variation of higher moments in a financial market with heterogeneous agents: an analytical approach. *J. Econ. Dyn. Control* 32 (1), 101–136. doi:10.1016/j.jedc.2006.12.014. <http://www.sciencedirect.com/science/article/pii/S0165188907000425>
- Alvarez-Ramirez, J., Alvarez, J., Solis, R., 2010. Crude oil market efficiency and modeling: insights from the multiscaling autocorrelation pattern. *Energy Econ.* 32 (5), 993–1000. doi:10.1016/j.eneco.2010.04.013. <https://www.sciencedirect.com/science/article/pii/S0140988310000691>
- Alvarez-Ramirez, J., Escarela-Perez, R., 2010. Time-dependent correlations in electricity markets. *Energy Econ.* 32 (2), 269–277. doi:10.1016/j.eneco.2009.05.008. <https://www.sciencedirect.com/science/article/pii/S0140988309000814>
- Bacry, E., Delour, J., Muzy, J.F., 2001. Multifractal random walk. *Phys. Rev. E* 64, 026103. doi:10.1103/PhysRevE.64.026103.
- Barde, S., 2016. Direct comparison of agent-based models of herding in financial markets. *J. Econ. Dyn. Control* 73, 329–353. doi:10.1016/j.jedc.2016.10.005. <http://www.sciencedirect.com/science/article/pii/S0165188916301622>
- Barde, S., 2017. A practical, accurate, information criterion for Nth order Markov processes. *Comput. Econ.* 50 (2), 281–324. doi:10.1007/s10614-016-9617-9.
- Barunik, J., Aste, T., Matteo, T.D., Liu, R., 2012. Understanding the source of multifractality in financial markets. *Physica A* 391 (17), 4234–4251. doi:10.1016/j.physa.2012.03.037. <http://www.sciencedirect.com/science/article/pii/S0378437112002890>
- Barunik, J., Kukacka, J., 2015. Realizing stock market crashes: stochastic cusp catastrophe model of returns under time-varying volatility. *Quant. Finance* 15 (6), 959–973. doi:10.1080/14697688.2014.950319.
- Beran, J., 1994. *Statistics for long-Memory processes*. Monographs on Statistics and Applied Probability, vol. 61. Chapman and Hall, New York.
- Bornholdt, S., 2001. Expectation bubbles in a spin model of markets: intermittency from frustration across scales. *Int. J. Modern Phys. C* 12 (5), 667–674.
- Brock, W.A., Hommes, C.H., 1997. A rational route to randomness. *Econometrica* 65 (5), 1059–1095.
- Brock, W.A., Hommes, C.H., 1998. Heterogeneous beliefs and routes to chaos in a simple asset pricing model. *J. Econ. Dyn. Control* 22, 1235–1274.
- Buonocore, R.J., Aste, T., Di Matteo, T., 2016. Measuring multiscaling in financial time-series. *Chaos Soliton. Fractals* 88, 38–47. doi:10.1016/j.chaos.2015.11.022.
- Buonocore, R.J., Aste, T., Di Matteo, T., 2017. Asymptotic scaling properties and estimation of the generalized Hurst exponents in financial data. *Phys. Rev. E* 95, 042311. doi:10.1103/PhysRevE.95.042311.
- Calvet, L., Fisher, A., 2001. Forecasting multifractal volatility. *J. Econom.* 105 (1), 27–58.
- Calvet, L., Fisher, A., 2002. Multifractality in asset returns: theory and evidence. *Rev. Econ. Stat.* 84, 381–406.
- Calvet, L., Fisher, A., 2008. *Multifractal volatility: Theory, forecasting, and pricing*. Academic Press.
- Calvet, L.E., Fisher, A.J., 2007. Multifrequency news and stock returns. *J. Financ. Econ.* 86 (1), 178–212. doi:10.1016/j.jfneco.2006.09.001. <https://www.sciencedirect.com/science/article/pii/S0304405X07000906>
- Calvet, L.-E., Grandmont, J.-M., Lemaire, I., 2018. Aggregation of heterogeneous beliefs, asset pricing, and risk sharing in complete financial markets. *Res. Econ.* 72 (1), 117–146. doi:10.1016/j.rie.2017.01.002. <https://www.sciencedirect.com/science/article/pii/S1090944316302794>
- Chen, S.-H., Chang, C.-L., Du, Y.-R., 2012. Agent-based economic models and econometrics. *Knowl. Eng. Rev.* 27, 187–219. doi:10.1017/S0269888912000136.
- Chen, W., Zhuang, J., Yu, W., Wang, Z., 2009. Measuring complexity using fuzzyen, apen, and sampen. *Med. Eng. Phys.* 31 (1), 61–68. doi:10.1016/j.medengphy.2008.04.005. <https://www.sciencedirect.com/science/article/pii/S1350453308000726>
- Chen, Z., Lux, T., 2018. Estimation of sentiment effects in financial markets: a simulated method of moments approach. *Comput. Econ.* 52 (3), 711–744. doi:10.1007/s10614-016-9638-4.
- Cobb, L., 1981. Parameter estimation for the cusp catastrophe model. *Behav. Sci.* 26 (1), 75–78. doi:10.1002/bs.3830260107.
- Cont, R., 2001. Empirical properties of asset returns: stylized facts and statistical issues. *Quant. Finance* 1 (2), 223–236. doi:10.1080/1713665670.
- Cont, R., Bouchaud, J.-P., 2000. Herd behavior and aggregate fluctuations in financial markets. *Macroecon. Dyn.* 4 (2), 170.196. doi:10.1017/S1365100500015029.
- Di Matteo, T., 2007. Multi-scaling in finance. *Quant. Finance* 7(1), 21–36.
- Di Matteo, T., Aste, T., Dacorogna, M.M., 2005. Long-term memories of developed and emerging markets: using the scaling analysis to characterize their stage of development. *J. Bank. Finance* 29, 827–851.
- Dieci, R., He, X.-Z., 2018. Heterogeneous Agent Models in Finance. In: Hommes, C., LeBaron, B. (Eds.), *Handbook of computational economics*, chapter 5. In: *Handbook of Computational Economics*, vol. 4. Elsevier, pp. 257–328. doi:10.1016/bs.hescom.2018.03.002. <http://www.sciencedirect.com/science/article/pii/S157400211830008X>
- Fagiolo, G., Guerini, M., Lamperti, F., Moneta, A., Roventini, A., 2019. Validation of agent-based models in economics and finance. In: Beisbart, C., Saam, N.J. (Eds.), *Computer Simulation Validation: Fundamental Concepts, Methodological Frameworks, and Philosophical Perspectives*. Springer International Publishing, pp. 763–787. doi:10.1007/978-3-319-70766-2_31.
- Fagiolo, G., Moneta, A., Windrum, P., 2007. A critical guide to empirical validation of agent-based models in economics: methodologies, procedures, and open problems. *Comput. Econ.* 30 (3), 195–226. doi:10.1007/s10614-007-9104-4.
- Franke, R., Westerhoff, F., 2011. Estimation of a structural stochastic volatility model of asset pricing. *Comput. Econ.* 38 (1), 53–83. doi:10.1007/s10614-010-9238-7.
- Franke, R., Westerhoff, F., 2016. Why a simple herding model may generate the stylized facts of daily returns: explanation and estimation. *J. Econ. Interact. Coordinat.* 11 (1), 1–34. doi:10.1007/s11403-014-0140-6.
- Gaunersdorfer, A., Hommes, C., 2007. A nonlinear structural model for volatility clustering. In: Teyssi re, G., Kirman, A.P. (Eds.), *Long Memory in Economics*. Springer Berlin Heidelberg, Berlin, Heidelberg, pp. 265–288. doi:10.1007/978-3-540-34625-8_9.
- Gaunersdorfer, A., Hommes, C.H., Wagener, F.O.O., 2008. Bifurcation routes to volatility clustering under evolutionary learning. *J. Econ. Behav. Org.* 67 (1), 27–47. doi:10.1016/j.jebo.2007.07.004. <http://www.sciencedirect.com/science/article/pii/S0167268107001588>
- Ghoshhadze, J., Lux, T., 2016. Bringing an elementary agent-based model to the data: estimation via GMM and an application to forecasting of asset price volatility. *J. Empiric. Finance* 37, 1–19. doi:10.1016/j.jempfin.2016.02.002. <http://www.sciencedirect.com/science/article/pii/S0927539816300093>
- Gilli, M., Winker, P., 2003. A global optimization heuristic for estimating agent based models. *Comput. Stat. Data Anal.* 42, 299–312.
- Gonzales Andino, S.L., Grave de Peralta Menendez, R., Thut, G., Spinelly, L., Blanke, O., Michel, C.M., Seeck, M., Landis, T., 2000. Measuring the complexity of time series: an application to neurophysiological signals. *Hum. Brain Mapp.* 11, 46–57.
- Grazzini, J., Richiardi, M., 2015. Estimation of ergodic agent-based models by simulated minimum distance. *J. Econ. Dyn. Control* 51, 148–165. doi:10.1016/j.jedc.2014.10.006. <http://www.sciencedirect.com/science/article/pii/S0165188914002814>
- Grazzini, J., Richiardi, M.G., Tsionas, M., 2017. Bayesian estimation of agent-based models. *J. Econ. Dyn. Control* 77, 26–47. doi:10.1016/j.jedc.2017.01.014. <http://www.sciencedirect.com/science/article/pii/S0165188917300222>
- Hommes, C.H., 2006. Heterogeneous Agent Models in Economics and Finance. In: Tesfatsion, L., Judd, K.L. (Eds.), *Handbook of computational economics*, chapter 23. In: *Handbook of Computational Economics*, vol. 2. Elsevier, pp. 1109–1186. doi:10.1016/S1574-0021(05)02023-X. <http://www.sciencedirect.com/science/article/pii/S157400210502023X>
- Ivanov, P., Nunes Amaral, L.A., Goldberger, A.L., Havlin, S., Rosenblum, M.G., Stanley, H.E., Struzik, Z.R., 2001. From 1/f noise to multifractal cascades in heartbeat dynamics. *Chaos* 11, 641–652.
- Jiang, Z.-Q., Xie, W.-J., Zhou, W.-X., Sornette, D., 2019. Multifractal analysis of financial markets: a review. *Rep. Prog. Phys.* 82, 125901.
- Jiang, Z.-Q., Zhou, W.-X., 2008. Multifractality in stock indexes: fact or fiction? *Physica A* 387, 3605–3614.
- Kantelhardt, J., Zschiegner, S., Koscielny-Bunde, E., Bunde, A., Havlin, S., Stanley, E., 2002. Multifractal detrended fluctuation analysis of nonstationary time series. *Physica A* 316(1–4), 87–114.
- Kantelhardt, J.W., 2009. *Encyclopedia of complexity and systems science*. Springer-Verlag New York, pp. 3754–3779.

- Kantelhardt, J.W., Koscielny-Bunde, E., Rego, H.H.A., Havlin, S., Bunde, A., 2001. Detecting long-range correlations with detrended fluctuation analysis. *Physica A* 295 (3), 441–454. doi:10.1016/S0378-4371(01)00144-3.
- Kirman, A., 1991. Money and financial markets. In: Taylor, M. (Ed.), *Money and Financial Markets*, pp. 354–368. Macmillan, New York, USA, pp. 354–368).
- Kirman, A., 1993. Ants, rationality, and recruitment. *Q. J. Econ.* 108 (1), 137–156.
- Kristoufek, L., Vosvrda, M., 2018. Herding, minority game, market clearing and efficient markets in a simple spin model framework. *Commun. Nonlinear Sci. Numer. Simul.* 54, 148–155. doi:10.1016/j.cnsns.2017.05.025. <http://www.sciencedirect.com/science/article/pii/S1007570417301867>
- Kukacka, J., Barunik, J., 2013. Behavioural breaks in the heterogeneous agent model: the impact of herding, overconfidence, and market sentiment. *Physica A* 392 (23), 5920–5938. doi:10.1016/j.physa.2013.07.050. <http://www.sciencedirect.com/science/article/pii/S0378437113006602>
- Kukacka, J., Barunik, J., 2017. Estimation of financial agent-based models with simulated maximum likelihood. *J. Econ. Dyn. Control* 85, 21–45.
- Kukacka, J., Kristoufek, L., 2020. Do 'complex' financial models really lead to complex dynamics? agent-based models and multifractality. *J. Econ. Dyn. Control* 113, 103855. doi:10.1016/j.jedc.2020.103855. <http://www.sciencedirect.com/science/article/pii/S0165188920300257>
- Lamperti, F., 2018a. Empirical validation of simulated models through the GSL-div: an illustrative application. *J. Econ. Interact. Coordinat.* 13 (1), 143–171. doi:10.1007/s11403-017-0206-3.
- Lamperti, F., 2018b. An information theoretic criterion for empirical validation of simulation models. *Econometric. Stat.* 5, 83–106. doi:10.1016/j.ecosta.2017.01.006. <http://www.sciencedirect.com/science/article/pii/S2452306217300084>
- Lamperti, F., Roventini, A., Sani, A., 2018. Agent-based model calibration using machine learning surrogates. *J. Econ. Dyn. Control* 90, 366–389. doi:10.1016/j.jedc.2018.03.011. <http://www.sciencedirect.com/science/article/pii/S0165188918301088>
- LeBaron, B., 2006. Chapter 24: Agent-based Computational Finance. In: Tesfatsion, L., Judd, K.L. (Eds.), *Handbook of computational economics*. In: *Handbook of Computational Economics*, vol. 2. Elsevier, pp. 1187–1233. doi:10.1016/S1574-0021(05)02024-1.
- LeBaron, B., Tesfatsion, L., 2008. Modeling macroeconomics as open-ended dynamic systems of interacting agents. *Am. Econ. Rev.* 98 (2), 246–250.
- Lee, J.S., Filatova, T., Ligmann-Zielinska, A., Hassani-Mahmooei, B., Stonedahl, F., Lorscheid, I., Voinov, A., Polhill, G., Sun, Z., Parker, D.C., 2015. The complexities of agent-based modeling output analysis. *J. Artif. Soc. Soc. Simul.* 18 (4).
- Liu, R., Di Matteo, T., Lux, T., 2008. Multifractality and long-range dependence of asset returns: the scaling behavior of the Markov-switching multifractal model with lognormal volatility components. *Adv. Complex Syst.* 11, 669–684.
- Lopes, R., Betrouni, N., 2009. Fractal and multifractal analysis: a review. *Med. Image Anal.* 13 (4), 634–649.
- Lucas Jr., R.E., 1978. Asset prices in an exchange economy. *Econometrica* 46, 1429–1445.
- Lux, T., 2004. Detecting multifractal properties in asset returns: the failure of the "scaling estimator". *Int. J. Modern Phys. C* 15 (04), 481–491. doi:10.1142/S0129183104005887.
- Lux, T., 2018. Estimation of agent-based models using sequential monte carlo methods. *J. Econ. Dyn. Control* 91, 391–408. doi:10.1016/j.jedc.2018.01.021. <http://www.sciencedirect.com/science/article/pii/S0165188918300356>
- Lux, T., Ausloos, M., 2002. Market fluctuations I: Scaling, multiscaling, and their possible origins. In: *The Science of Disasters: Climate Disruptions, Heart Attacks, and Market Crashes*. Springer Berlin Heidelberg, Berlin, Heidelberg, pp. 372–409.
- Lux, T., Kaizoji, T., 2007. Forecasting volatility and volume in the tokyo stock market: long memory, fractality and regime switching. *J. Econ. Dyn. Control* 31 (6), 1808–1843.
- Lux, T., Zwinkels, R.C.J., 2018. Chapter 8 - Empirical Validation of Agent-based Models. In: Hommes, C., LeBaron, B. (Eds.), *Handbook of computational economics*. In: *Handbook of Computational Economics*, vol. 4. Elsevier, pp. 437–488. doi:10.1016/bs.hescom.2018.02.003. <https://www.sciencedirect.com/science/article/pii/S1574002118300030>
- Mandelbrot, B., Van Ness, J.W., 1968. Fractional brownian motions, fractional noises and applications. *SIAM Rev.* 10 (4), 422–437.
- Mandes, A., Winker, P., 2017. Complexity and model comparison in agent based modeling of financial markets. *J. Econ. Interact. Coordinat.* 12 (3), 469–506.
- Marks, R.E., 2013. Validation and model selection: three similarity measures compared. *Complex. Econ.* 2 (1), 41–61.
- Morales, R., Di Matteo, T., Gramatica, R., Aste, T., 2012. Dynamical generalized Hurst exponent as a tool to monitor unstable periods in financial time series. *Physica A* 391, 3180–3189.
- Peng, C., Buldyrev, S., Goldberger, A., Havlin, S., Simons, M., Stanley, H., 1993. Finite-size effects on long-range correlations: implications for analyzing DNA sequences. *Phys. Rev. E* 47(5), 3730–3733.
- Platt, D., 2020. A comparison of economic agent-based model calibration methods. *J. Econ. Dyn. Control* 113, 103859. doi:10.1016/j.jedc.2020.103859. <http://www.sciencedirect.com/science/article/pii/S0165188920300294>
- Podobnik, B., Jiang, Z.-Q., Zhou, W.-X., Stanley, H.E., 2011. Statistical tests for power-law cross-correlated processes. *Phys. Rev. E* 84, 066118.
- Podobnik, B., Stanley, H.E., 2008. Detrended cross-correlation analysis: a new method for analyzing two nonstationary time series. *Phys. Rev. Lett.* 100, 084102.
- Polach, J., Kukacka, J., 2019. Prospect theory in the heterogeneous agent model. *J. Econ. Interact. Coordinat.* 14 (1), 147–174. doi:10.1007/s11403-018-0219-6.
- Qian, X.-Y., Liu, Y.-M., Jiang, Z.-Q., Podobnik, B., Zhou, W.-X., Stanley, H.E., 2015. Detrended partial cross-correlation analysis of two nonstationary time series influenced by common external forces. *Phys. Rev. E* 91, 062816.
- Rak, R., Grech, D., 2018. Quantitative approach to multifractality induced by correlations and broad distribution of data. *Physica A* 508, 48–66.
- Recchioni, M.C., Tedeschi, G., Gallegati, M., 2015. A calibration procedure for analyzing stock price dynamics in an agent-based framework. *J. Econ. Dyn. Control* 60, 1–25.
- Schmitt, N., 2020. Heterogeneous expectations and asset price dynamics. *Macroecon. Dyn.* 1–31. doi:10.1017/S1365100519000774.
- Schmitt, N., Westerhoff, F., 2017. Heterogeneity, spontaneous coordination and extreme events within large-scale and small-scale agent-based financial market models. *J. Evolut. Econ.* 27 (5), 1041–1070. doi:10.1007/s00191-017-0504-x.
- Shimizu, Y., Thurner, S., Ehrenberger, K., 2002. Multifractal spectra as a measure of complexity in human posture. *Fractals* 10, 103–116.
- Siokis, F.M., 2017. Financial markets during highly anxious time: multifractal fluctuations in asset returns. *Fractals* 25 (03), 1750032. doi:10.1142/S0218348X17500323.
- Thom, R., 1975. *Structural stability and morphogenesis*. Benjamin, New York.
- Torres, M.E., Gamero, L.G., 2000. Relative complexity changes in time series using information measures. *Physica A* 286 (3), 457–473. doi:10.1016/S0378-4371(00)00309-5. <https://www.sciencedirect.com/science/article/pii/S0378437100003095>
- Welch, B.L., 1947. The generalization of 'Student's' problem when several different population variances are involved. *Biometrika* 34 (1/2), 28–35. <http://www.jstor.org/stable/2332510>
- Windrum, P., Fagiolo, G., Moneta, A., 2007. Empirical validation of agent-based models: alternatives and prospects. *Journal of Artificial Societies and Social Simulation* 10 (2), 8. <http://jasss.soc.surrey.ac.uk/10/2/8.html>
- Zeeman, E.C., 1974. On the unstable behaviour of stock exchanges. *Journal of Mathematical Economics* 1, 39–49.
- Zhou, W.-X., 2009. The components of empirical multifractality in financial returns. *Europhys Lett* 88 (2), 28004. doi:10.1209/0295-5075/88/28004.